

**Flammability Limits,
Ignition Energy and Flame Speeds
in H₂-CH₄-NH₃-N₂O-O₂-N₂ Mixtures**

short title: Flammability, Ignition Energy and Flame Speed

U.J. Pfahl, M.C. Ross and J.E. Shepherd

Graduate Aeronautical Laboratories
California Institute of Technology
Pasadena, CA 91125, USA

K.O. Pasamehmetoglu and C. Unal

Technology & Safety Assessment Division
Los Alamos National Laboratory
Los Alamos, NM 87545, USA

submitted as *full-length article* in:
Combustion and Flame

Revised version of March 25, 2000.

corresponding author:

Joseph E. Shepherd
Caltech, 105-50
Pasadena, CA 91125

Phone: 626-395-3283
Fax: 626-449-2677
E-Mail: jeshep@galcit.caltech.edu

Flammability Limits, Ignition Energy and Flame Speeds in $\text{H}_2\text{-CH}_4\text{-NH}_3\text{-N}_2\text{O-O}_2\text{-N}_2$ Mixtures

U.J. Pfahl, M.C. Ross and J.E. Shepherd

Graduate Aeronautical Laboratories
California Institute of Technology
Pasadena, CA 91125, USA

K.O. Pasamehmetoglu and C. Unal

Technology & Safety Assessment Division
Los Alamos National Laboratory
Los Alamos, NM 87545, USA

Abstract

Experiments on flammability limits, ignition energies, and flame speeds were carried out in a 11.25- and a 400-liter combustion vessel at initial pressures and temperatures of 100 kPa and 295 K, respectively. Flammability maps of hydrogen-nitrous oxide-nitrogen, methane-nitrous oxide-nitrogen, ammonia-nitrous oxide-nitrogen, and ammonia-nitrous oxide-air, as well as lean flammability limits of various hydrogen-methane-ammonia-nitrous oxide-oxygen-nitrogen mixtures were determined. Ignition energy bounds of methane-nitrous oxide, ammonia-nitrous oxide, and ammonia-nitrous oxide-nitrogen mixtures have been determined and the influence of small amounts of oxygen on the flammability of methane-nitrous oxide-nitrogen mixtures has been investigated. Flame speeds have been measured and laminar burning velocities have been determined for ammonia-air-nitrous oxide and various hydrogen-methane-ammonia-nitrous oxide-oxygen-nitrogen mixtures. Lower and upper flammability limits (mixing fan on, turbulent conditions) for ignition energies of 8 J are: $\text{H}_2\text{-N}_2\text{O}$: 4.5~5.0% H_2 (LFL), 76~80% H_2 (UFL); $\text{CH}_4\text{-N}_2\text{O}$: 2.5~3.0% CH_4 (LFL), 43~50% CH_4 (UFL); $\text{NH}_3\text{-N}_2\text{O}$: 5.0~5.2% NH_3 (LFL), 67.5~68% NH_3 (UFL). Inerting concentrations are: $\text{H}_2\text{-N}_2\text{O-N}_2$: 76% N_2 ; $\text{CH}_4\text{-N}_2\text{O-N}_2$: 70.5% N_2 ; $\text{NH}_3\text{-N}_2\text{O-N}_2$: 61% N_2 ; $\text{NH}_3\text{-N}_2\text{O-air}$: 85% air. Flammability limits of methane-nitrous oxide-nitrogen mixtures show no pronounced dependence on small amounts of oxygen (< 5%). Generally speaking, flammable gases with large initial amounts of nitrous oxide or ammonia show a strong dependence of flammability limits on ignition energy.

1 Introduction

The nuclear wastes stored in underground storage tanks at Hanford site are known to generate, by complex chemical reactions, a flammable gas mixture that comprises mainly hydrogen, ammonia, methane, and nitrous oxide. The flammable gas mixture generated in the waste is periodically released into the dome space of storage tanks with various quantities. Tank 101-SY has been found to release concentrations greater than lower flammability limits (LFL) of hydrogen during episodic gas release events. In the unlikely event that an ignition source were present during episodic gas releases, a burn or explosion could occur. An ignition of the flammable gas mixture is a significant safety hazard and can result in tank dome pressures exceeding structural limits, which in turn could result in unacceptable structural damage to the tanks and release of radioactive material. A mixer pump is installed into Tank 101-SY to eliminate the episodic releases as a part of the proposed mitigation strategy. Sullivan et al. [1] systematically assesses the safety issues associated with the installation, operation and removal of the mixer pump in Tank 101-SY. They identify several representative postulated flammable gas burn accident scenarios. The characterization of combustion behavior of $\text{H}_2\text{-CH}_4\text{-NH}_3\text{-N}_2\text{O-O}_2\text{-N}_2$ mixtures was necessary to assess the consequences of burn accidents. The combustion behavior of $\text{H}_2\text{-CH}_4\text{-NH}_3\text{-N}_2\text{O-O}_2\text{-N}_2$ mixtures is not well understood. Particularly, there is a lack of data on the flammability limits in terms of ignition energies and flame speeds at various concentrations.

The goals of this study are to experimentally characterize the combustion behavior of hydrogen, methane and ammonia with nitrous oxide or air. Our approach is to carry out laboratory experiments with a spark ignition system in closed vessels of 11.25 and 400 liter capacity. Measurements of pressure vs. time and video recordings of schlieren visualization were used to determine the ignition limits as a function of stored energy in spark discharge system. Our study determines flammability limits empirically by finding the limiting concentrations of reactants for which we can initiate combustion and have it propagate throughout the vessel.

Traditional evaluations of explosion hazards rely on comparing the fuel concentration to the measured flammability limit. However, the flammability limit depends on the choice of ignition method and sample preparation. Consequently, different methods of measuring flammability have been devised such as the flashpoint test [2], spark ignition [3], temperature limit method [4], and concentration limit method [5]. Each of these uses different ignition methods: an open pilot flame in the flashpoint test; a capacitive spark in the spark ignition test; an electrically heated fuse-wire in the temperature limit test; and either a fuse wire or an electric arc in the concentration limit method. The most commonly used method of all, the flammability limit tube developed at the Bureau of Mines [6, 7, 8], has never been standardized. This method uses various ignition sources; one commonly employed is a quasi-continuous arc produced by a neon-sign transformer (20 kV, 30 mA) across a 0.25-in gap. Our experience [9, 10] at Caltech is that results obtained with a 100-J spark igniter in a closed vessel are similar to those obtained with

the Bureau Mines apparatus using a neon-sign transformer arc. In the present study, stored energies of up to 8 J were used since this level is reasonable to achieve without creating the large amount of electrical noise that a 100 J spark produces.

Various ideas have been advanced to explain the phenomena of flammability and the relationship to tests developed in the process industries to determine flammability limits. It is important to note the distinction between the use of the term “flammability limit” by the safety community and by the combustion basic research community. Safety studies are concerned with experimentally determining limiting concentrations, beyond which combustion can be assured not to occur. The experimental determination of such limits is inextricably intertwined with the apparatus, including method of ignition, the test protocol, and the criteria for determining when ignition has occurred. Basic researchers prefer to think of limits in the abstract. Starting with Spalding [11], the generally accepted definition has become that the flammability limit is that state at which steady propagation of a one-dimensional premixed flame fails to be possible. The theoretical determination of a limit defined in this fashion is likewise tied a specific configuration, a chemical kinetic model, diffusive and radiative transport models, and numerical solution methods. Recently there has been some progress towards connecting these two approaches to flammability.

From a theoretical point of view, limits arise because mechanisms such as chain-terminating reaction steps, energy loss by radiation, and preferential diffusion eventually dominate the energy-releasing chemical reactions and cause extinction at the flammability limit. The idea of heat losses creating a limiting condition was first advanced by Spalding [11] but testing this notion quantitatively had to wait for the development of detailed reaction mechanisms and flame structure computation methods. Law and Egofopolous [12] showed that turning points in one-dimensional steady laminar flame computations with a simplified radiative loss model correlated reasonably well with known experimental limits for lean methane-air and rich hydrogen-air mixtures. More recent studies [13] show that the situation is substantially more complex when the combined effects of strain and radiation are considered, particularly for mixtures with Lewis numbers less than unity. The “doubly-infinite” and “twin-flame” configurations considered in these studies is ideal for numerical simulation but quite far from the unsteady, multi-dimensional flame kernels in confined vessels that are utilized in most flammability tests.

Bui-Pham et al. [14] have made a detailed comparison of limits determined experimentally with spark and chemical igniters to predictions based on adiabatic, steady, laminar flame computations for the rich flammability limit of $\text{CH}_3\text{OH}/\text{CO}/\text{diluent}$ mixtures in O_2 . Two simple ideas were examined: 1) a limit flame speed of 5 cm/s; and, 2) equality of primary chain termination rates and radical production rates. Although the predicted trends for critical oxygen concentration with pressure and diluent type were qualitatively correct, the quantitative values were not. Unsteady computations of spherically-symmetric ignition were quantitatively more accurate but very computationally expensive. Furthermore, as Bui-Pham et al. point out, intrinsic flammability limits and ignitability appear to be two distinct phenomena. The most striking results was the

existence of mixtures that could be ignited and burned completely although they were apparently outside the theoretically determined flammability limit. Clearly, such results indicate that the prediction of flammability is an active research area and substantial gaps remain between present theoretical understanding and industrial practice.

Experimental flammability limits of the individual fuels in air are fairly well characterized. Available data on limits are summarized in Table 1. However, there are some peculiar aspects to these fuel–oxidizer combinations, particularly with mixtures containing nitrous oxide. N_2O decomposes slowly at low temperatures (Arrhenius activation energy of ~ 251 kJ/mol [15]) but is extremely exothermic. N_2O can behave as an explosive if the ignition stimulus is large enough and there are sufficient H atoms present to catalyze the decomposition. However, for very low temperature flames, the N_2O does not appear to react at all [15, 16]. Mixtures of ammonia and air burn very slowly and in many situations are considered to be nonflammable, but mixtures of NH_3 and N_2O appear to react much more rapidly. The reaction mechanism of NH_3 and N_2O is particularly uncertain. Hydrogen has a very large flammability range and unusually high flame speeds.

Fuel	LFL		ST	UFL	Inert (N_2)
	UPL	DPL			
H_2	4	8	29.6	75	70
CH_4	5		9.5	15	37
NH_3	15	18	22	28	15

Table 1: Flammability limits of fuel–air mixtures at normal temperature and pressure. Amounts are given in volume %. LFL: lower flammability limit, ST: volume % fuel for a stoichiometric mixture, UFL: upper flammability limit, inert: volume % nitrogen to inert the mixture, UPL: upward propagation limit, DPL: downward propagation limit

Flammability of fuels in N_2O is not as well characterized as in air. At the time we started this study, no information was available on CH_4 limits and the data available for NH_3 were quite limited. Understanding of flammability in binary and ternary fuel mixtures (H_2 - NH_3 - CH_4) is rudimentary. The most common assumption is known as Le Chatelier’s Rule [17]. The effect of multiple oxidizers (O_2 , N_2O) on flammability limits is not well understood.

In the present study we have concentrated on measuring flammability maps of hydrogen–nitrous oxide–nitrogen, methane–nitrous oxide–nitrogen, ammonia–nitrous oxide–nitrogen and ammonia–nitrous oxide–air mixtures at an initial pressure of 100 kPa and an initial temperature of about 22°C, even though the gas temperatures in the waste storage tanks at Hanford vary between 20 and 60°C, which could have a strong influence on the flammability limits [18]. We have also investigated the influence of ignition energy on flammability limits for these mixtures and for seven different hydrogen–methane–ammonia–nitrous

oxide–nitrogen mixtures A - G, which are given in Table 2. These mixtures were chosen with respect to explosion and detonation hazards at the waste storage tanks at Hanford Site, Washington State [1, 19]. Mixture G represents the best estimated gas composition of flammable gas mixture of Tank 101-SY. The other mixture recipes were considered to study the composition effects parametrically. Finally, laminar burning velocities were obtained for ammonia–air–nitrous oxide mixtures and for mixtures A - G in air.

Mixture	H ₂ (vol %)	N ₂ O (vol %)	NH ₃ (vol %)	CH ₄ (vol %)	N ₂ (vol %)
A	42	36	21	1	0
B	35	35	30	0	0
C	25	25	50	0	0
D	16.7	33.3	50	0	0
E	40	40	0	20	0
F	35	35	20	10	0
G	29	24	11	1	35

Table 2: Fuel blends A - G considered in the present study.

2 Apparatus

The present experiments were done in two different constant volume combustion vessels. The smaller vessel with a volume of 11.25 liters was constructed of steel slabs and formed a rectangular chamber with internal dimensions of 190 mm × 203 mm × 305 mm. This facility including its instrumentation is shown in Fig. 1. The larger vessel had a volume of approximately 400 liters. The gas handling and exhaust systems were identical for both vessels. Furthermore, both vessels were equipped with similar instrumentation to observe flame propagation and to record pressure and temperature development.

Fig. 1

The vessels were filled with a mixture of gases using partial pressures to determine composition. Because of different hazards, especially while using ammonia, several safety features (check valves, gas detectors, logic valve control circuits) were necessary while operating the facilities. The products were exhausted through a treatment system following combustion. Again, special precautions, described by Ross and Shepherd [19], were taken when using ammonia to prevent gas releases.

The combustion facilities were instrumented with pressure and temperature sensors. The static pressure gauge to meter the initial pressures of the reactants and the final pressure of the products was a Heise, model 901A, digital pressure indicator with a range from 0 to 250 kPa absolute and an accuracy of ±0.18 kPa. A dynamic Kulite Semiconductor Pressure Gauge, model XTME-190-250A, was used to monitor the explosion

pressure. This is a piezoresistive type transducer which has a combined nonlinearity, hysteresis and repeatability of 2.5 kPa. This transducer was protected by two porous metal frits, which are sufficient to shield the transducer from temperature but do not affect the pressure reading. A thermocouple Omega K type with a 3.2 mm metal sheath was installed above the center of the spark source (see Fig. 1). Each wire was 24 AWG, and the weld bead size was approximately 1.5 mm. An Omega model DP462 electronic cold-junction and temperature readout was used to convert the thermocouple output to temperature. The pressure and temperature signals were recorded by Labview Data Acquisition Software running on a personal computer. Furthermore, both vessels were equipped with 25 mm thick glass windows with a clear aperture of 117 mm in diameter (see Figs. 1 and 2). Through these windows, a color-schlieren video-system was used to observe the flame initiation and propagation (see Figs. 4 - 6). Figure 2 shows a schematic diagram of the optical set-up of the color-schlieren video-system.

Fig. 2

An electric spark was used to initiate the flame. In both vessels the spark gap (see Fig. 1: 2-6 mm depending on the gas composition) was positioned in the center of the vessel and the electrodes passed through Teflon insulators on the sides of the vessel. The power for the spark was provided by a 0.5 μ F capacitor charged by a Hipotronics 15 kV (maximum) power supply. The discharge across the gap was triggered by a 30 kV pulse (low current) from an EG&G TM-11A power supply. Figure 3 shows a schematic diagram of the electrical circuit of the spark ignition system. The circuit was motivated by the design described by Ronney [20].

The duration of the main pulse is controlled by the time constant (RC product) and the discharge characteristics. For a low-impedance discharge, the time constant is most important. For the circuit of Fig. 3, the characteristic discharge time is about 100 μ s. The discharge time of the trigger pulse itself is on the order of 1 μ s. In the present study, the ignition energy reported is actually the energy stored in the capacitor used to create the electrical discharge. In our arrangement, the residual energy remaining in the capacitor after the discharge was less than 1% [10]. However, due to the finite impedance of the circuit and the complex nature of electrical arcs, it is not possible to draw any conclusions about the amount of energy deposited into the arc. In order to do that, it would be necessary to determine the actual energy dissipated within the arc which requires measuring the voltage $v(t)$ across the arc and current $i(t)$ through the arc as a function of time. Various arrangements have been proposed to do that; a review is given by [21]. However, unless the discharge parameters are chosen carefully to minimize phase errors in current and voltage, the energy measurement will be highly inaccurate.

Fig. 3

Investigations were carried out under quiescent or turbulent gas conditions. The data in Fig. 8, 9, 10, 11, 12, 14, 15, 16, 17, were all obtained in the the smaller vessel (11.25 liters) with the fan on the top running. The turbulence intensity was characterized in this vessel near the ignition location. The data in Fig. 13, 19 and some data of 20 (A-D) were obtained in the larger vessel (400 l) but without the fan running. The data sets E-F of Fig. 20 were obtained in the smaller vessel but with the fan not running.

The turbulence was produced by a single mixing fan with two blades, about 150 mm in diameter. The mixing fan was driven by a pulley drive (6.7:1 reduction) from a universal motor controlled by a speed control (light-dimmer switch). The shaft for the fan was connected to a magnetic torque transmitter which was located at the top of the 11.25 liter vessel (see Fig. 1) and at the side of the 400 liter vessel, respectively. Flow measurements with a single-component laser doppler anemometer (LDA) near the ignition location showed that mean flow \bar{u} and fluctuations u_{rms} increased with fan rotational speed. However, the turbulence intensity $u' = u_{rms}/\bar{u}$ was found to be relatively independent of the rotational speed between $u' = 0.24$ and $u' = 0.26$. Measurements at various locations also indicated that the turbulence intensity was relatively independent of position.

3 Results and Discussion

Flammability Limits

The flammability limits of a combustible mixture are those limiting compositions that will just support flame propagation when stimulated by an external ignition source. Identifying these limits is of great interest to the chemical industry and safety engineers, and compilations of flammability limits have been published by the Bureau of Mines [22, 18]. Although there is no widely accepted theoretical method of predicting flammability limits, there are a number of empirical rules and simple models [11], the classical results are summarized in Lewis and Von Elbe [23] and updated in the series of reports by Hertzberg [24]. The fuel type, mixture properties and mass diffusion of the deficient reactant are all factors [25] in defining the limiting composition.

Mixtures that are either too rich or too lean are not flammable. In the present study, we are concerned with fuel-lean as well as fuel-rich mixtures. Lower or lean flammability limits are known in the literature as LFL, upper or rich flammability limits are known as UFL. Flammability limits are determined by a variety of techniques, each of which yields a slightly different value of the limiting composition.

Further complications are the effect of ignition energy (see Section *Ignition Energies* below) and the buoyancy of the hot combustion products. The effect of buoyancy is to cause the initially spherical flame kernel, created by the spark, to rise and become distorted as it propagates outward. As a consequence, if the burning velocity is too low (less than about 5 cm/s), the flame is observed only to propagate upward. The gradients in the gas velocity induced by the rising flame also affect the flammability limit. The gradients and spherical expansion of the flame surface result in *flame stretch* which increases the burning rate if the Lewis number Le (ratio of thermal diffusivity to mass diffusivity of the deficient reactant) is less than one and decreases the burning rate if $Le > 1$.

Figures 4, 5, and 6 show different cases of flame propagation, which illustrate the

range of combustion phenomena observed in these experiments at the lean flammability limit: a typical laminar flame is shown in Fig. 4. This case is 20% NH_3 in air, the mixing fan is turned off (quiescent conditions). The flame front is smooth and spherical. A dimple produced by buoyancy is observed at the bottom of the flame in the last two frames. Figure 5 shows a frame sequence of a slightly leaner mixture, 18% NH_3 in air, but the mixing fan is turned on in this case (turbulent conditions). A highly wrinkled flame front is seen in all frames. Turbulent motion induced by the mixing fan has the effect of distorting and rapidly convecting the flame away from the ignition point. In contrast to an upward propagation flame at quiescent conditions, a mixing fan can result in combustion within the total volume of the vessel as long as the turbulence intensity is not so large that the flame is quenched. For richer mixtures, the instability of the flame results in a cellular structure visible as bright lines on the flame surface. This is observed in Fig. 6 for a quiescent burn of 20% of Mixture B (see Table 2) in air.

Fig. 4

The limiting composition at which upward propagation of the flame begins is referred to as the upward propagation limit (UPL) in the literature. The composition at which the transition from upward to downward propagation takes place is known as the downward propagation limit (DPL). In this study, we have determined propagation limits of various mixtures: hydrogen–nitrous oxide with nitrogen dilution, methane–nitrous oxide with nitrogen dilution and small amounts of oxygen (3 and 5%), ammonia–nitrous oxide with nitrogen and air dilution, hydrogen–ammonia–air, and seven different hydrogen–methane–ammonia–nitrous oxide–nitrogen–oxygen mixtures (see Table 2). All experiments were carried out at a total initial pressure of 100 kPa and an initial temperature of 295 K.

Fig. 5

Fig. 6

The mixing fan was running (turbulent conditions) during flame initiation and propagation for all flammability tests except those shown in Figs. 13, 19, and 20. The fan is expected to generate a mean flow but it is difficult to distinguish this effect from the buoyancy. The main effect of the fan is in providing sufficient convection so that relatively complete combustion occurs, enabling clear determination of the flammability limit. Otherwise, in many cases buoyancy causes an extended regime between upward and downward propagation limits, as shown in Fig. 13. The flammability limits measured with the fan running correspond to the upward propagation limit, which is a conservative estimate from the point of view of safety. The ignition source was the capacitor discharge unit described in Sections *Apparatus* and *Ignition Energies*. The spark ignition energy was 8 J.

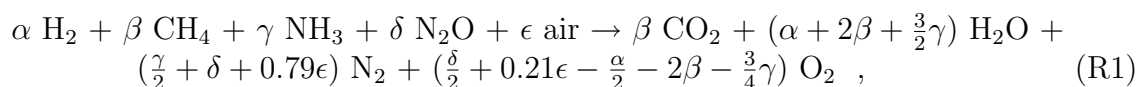
The most common assumption regarding flammability in binary and ternary fuel mixtures is that the limiting mole fractions X_i of each fuel species i obey Le Chatelier’s Rule [17]:

$$\sum_{\text{fuels}} \frac{X_i}{X_{i,LFL}} = 1 \quad \text{at mixture LFL} \quad (1)$$

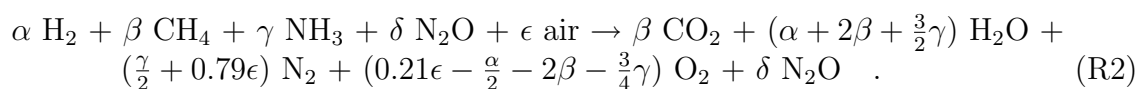
where $X_{i,LFL}$ is the limit concentration for a single fuel species i in the oxidizer-diluent mixture of interest. For many compounds mixed in oxygen or air, this rule is a reason-

able approximation. The physical reasoning behind this model is that the reactants are compatible in kinetic and transport properties, and independently compete for oxidizer within the flame front. It is not clear how to extend Le Chatelier's Rule to include the effect of multiple oxidizers such as O_2 and N_2O .

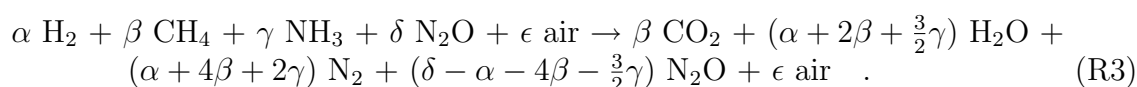
The major products for lean combustion of H_2 - CH_4 - NH_3 - N_2O -air mixtures are CO_2 , H_2O , and N_2 . If complete reaction of H_2 , CH_4 , and NH_3 occurs and all the N_2O decomposes, the overall reaction is:



where one mole of air has been approximated as $0.21 O_2 + 0.79 N_2$. If the N_2O does not react or decompose in the combustion process, which is expected for some of the lean mixtures (low temperatures) [16], the overall reaction will be



Finally, if the oxidation of the fuel occurs preferentially by N_2O rather than O_2 , this reaction is modified to



The first overall reaction R1 (full dissociation of N_2O) corresponds to complete equilibrium and would be predicted by usual thermodynamic equilibrium estimates [26]. However, equilibrium models, though useful for estimating thermodynamic properties of combustion systems, can not predict which oxidizer is preferred by the fuels in a multi-component system. Experimental measurements of the intermediate and product species are needed. Modeling based on detailed chemical kinetics and known elementary reaction rates is a valuable alternative and supplement to experiments, but not task of the present study.

Hydrogen–Nitrous Oxide–Nitrogen Mixtures

Numerous flammability studies have been conducted with hydrogen. Some of these studies, Smith and Linnett (1953) [27], Posthumus (1930) [28], van der Wal (1934) [29], and Scott et al. (1957) [30] have been carried out with N_2O as the oxidizer. The available data are shown in Fig. 7 together with the flammability limits of hydrogen–oxygen [22] and hydrogen–air–nitrogen mixtures [18, 31]. These data are all nominally obtained at a temperature of $25^\circ C$ and a pressure of 1 atm. Not shown in that plot are the H_2 - N_2O -air

mixture data of Cashdollar et al. (1992) [32] and Ross and Shepherd (1996) [19]. Note that the rich limit data of Posthumus are substantially below those of Smith and Linnett. This is apparently due to the low temperature/energy ignition source of Posthumus in comparison to the 20 J spark discharge used by Smith and Linnett. In general, ignition energy has a strong effect on flammability limits in mixtures containing large amounts of N_2O . The particular problem of ignition of very lean H_2-N_2O mixtures is discussed subsequently in Section *Ignition Energies*.

Fig. 7

Flammability limits were determined for $H_2-N_2O-N_2$ mixtures at 100 kPa and 295 K, the mixing fan was running during the tests. The results are shown in Fig. 8. The flammability limits of hydrogen–nitrous oxide mixtures occur at 4.5~5.0% (LFL) and 76~80% (UFL) hydrogen for ignition energies of approx. 8 J. Addition of 76% nitrogen (see Fig. 8) will inert the mixtures. Our results are in very good agreement to what was obtained by Smith and Linnett (1953) [27] for nitrogen dilution below 50%, but above 50% nitrogen dilution we observed a wider range of flammability than Posthumus [28] and a higher inerting nitrogen concentration. Posthumus had only very limited data in this region and his inerting concentration is not well defined.

Fig. 8

Methane–Nitrous Oxide–Nitrogen Mixtures

Flammability limits were determined for $CH_4-N_2O-N_2$ mixtures at 100 kPa and 295 K, the mixing fan was running during the test. The results are shown in Fig. 9. The flammability limits of methane–nitrous oxide mixtures occur at 2.5~3.0% (LFL) and 43~50% (UFL) methane for ignition energies of approx. 8 J. Addition of 70.5% nitrogen (see Fig. 9) will inert the mixtures. The corresponding methane partial pressure is 6.3 kPa. The present results are compared in Fig. 9 to previous results from the literature [18] for $CH_4-O_2-N_2$ mixtures. Previous results for CH_4-N_2O or $CH_4-N_2O-N_2$ mixtures were not available from the literature. The lower flammability limit shows a very smooth dependence (increase) on the amount of nitrogen dilution and a good correspondence to Zabetakis' results for $CH_4-O_2-N_2$, whereas the upper limit shifts to a smaller flammability region compared to $CH_4-O_2-N_2$ and shows a strong decrease with increasing nitrogen dilution.

Fig. 9

Influence of Small Amounts of Oxygen (3 - 5%) on the Flammability Limits of Methane–Nitrous Oxide–Nitrogen Mixtures

Figures 9 and 10 show no pronounced dependence of the flammability limits of methane–nitrous oxide–nitrogen mixtures on small amounts of oxygen. At 3 kPa oxygen addition, the maximum flammable nitrogen dilution does not shift (see Fig. 10). Substituting oxygen for nitrous oxide shifts the maximum flammable nitrogen dilution (inerting concentration) from 70.5 to about 85 kPa (5 kPa CH_4 and 10 kPa O_2). Zabetakis obtained 80 kPa nitrogen dilution as the inerting concentration for $CH_4-O_2-N_2$ mixtures at atmospheric pressure and 26°C [18]. The present results exceed this value due to turbulent

conditions (the mixing fan was on during the burn). Addition of 5 kPa oxygen at 0, 10, 40 and 47.5 kPa nitrogen dilution does not appreciably alter the flammability limits (see Fig. 9).

Fig. 10

Ammonia–Nitrous Oxide–Nitrogen Mixtures

Flammability studies have been conducted with ammonia by Fenton et al. (1995) [33], Armitage and Gray (1965) [34], Andrews and Gray (1964) [35], Buckley and Husa (1962) [36], van der Wal (1934) [29], Jorissen and Ongkiehong (1926) [37], and White (1922) [38]. We have made measurements with ammonia–nitrous oxide–nitrogen mixtures to determine lower and upper flammability limits and inerting concentrations. The present results are shown in Fig. 11. The flammability limits of ammonia–nitrous oxide mixtures occur at 5.0~5.2% (LFL) and 67.5~68% (UFL) ammonia for ignition energies of approx. 8 J. Addition of 61% N₂ (see Fig. 11: 10.5-16% NH₃, 28.5-23% N₂O) will inert the mixtures.

Fig. 11

Ammonia–Nitrous Oxide–Air Mixtures

In addition to our ammonia–nitrous oxide experiments with nitrogen dilution we performed further tests with air dilution. The results are shown in Fig. 11. Whereas the lower flammability limit is almost similar with air or nitrogen dilution up to 60% dilution, the upper flammability limit (fuel rich, oxygen lean) decreases less with increasing air dilution than with increasing nitrogen dilution. This results in a larger flammability limit and an inerting air concentration of 85% (see Fig. 12: 15% NH₃, 0% N₂O). All mixtures between 71 and 85% NH₃ (29-15% air, 0% N₂O) are flammable with ignition energies of approx. 8 J.

Fig. 12

Hydrogen–Ammonia–Air Mixtures

In this study, we examined the upward and downward propagation lean limits for the binary fuel H₂-NH₃. The concentration of H₂ was varied in 2% increments and the NH₃ in 1% increments. Using Le Chatelier's rule as a guide, the upward and downward propagation limits were bracketed. Results are shown in Fig. 13. The data symbols in this graph indicate the experimental conditions closest to the lean combustion phenomenon. The linear H₂-NH₃ relationship for the limits indicate that Le Chatelier's rule for binary mixtures is appropriate for this system.

Fig. 13

Hydrogen–Methane–Ammonia–Nitrous Oxide–Oxygen–Nitrogen Mixtures

Flammability limits of hydrogen, methane and ammonia as mixtures with nitrous oxide are presented above. In addition to these experiments, we performed flammability limit

tests with seven different hydrogen–methane–ammonia–nitrous oxide–nitrogen mixtures (see Table 2) in air. Mixture G represents the best estimated gas composition of flammable gas mixture of Tank 101-SY at Hanford site. The other mixture recipes were considered to study the composition effects parametrically. The initial conditions were: $p_0 = 100$ kPa, $T_0 = 295$ K, and ignition energy ≈ 8 J.

The fuel composition of mixture A is 42% H₂, 36% N₂O, 21% NH₃, and 1% CH₄. For this mixture, we observed downward propagation flames (fan off: quiescent conditions) above 15%, whereas with a mixing fan (turbulent conditions) the lean flammability limit was obtained between 8 and 10% mixture A.

The fuel composition of mixture B is 35% H₂, 35% N₂O, and 30% NH₃, it has a higher NH₃ to H₂ ratio than mixture A. For this mixture, we observed downward propagation flames (fan off: quiescent conditions) above 14%. The lean upward propagation limit, determined by the video color schlieren system, was about 9% mixture B.

The fuel composition of mixture C is 25% H₂, 25% N₂O, and 50% NH₃. The lean upward propagation limit is 10%, 9% and lower concentrations of mixture C resulted in no flame detection by the schlieren system. The downward propagation limit was observed around 16%.

The fuel composition of mixture D is 16.7% H₂, 33.3% N₂O, and 50% NH₃. This mixture contains a NH₃/H₂ ratio of 3:1. Combustion peak pressure results indicate a lean downward propagation limit of 20%. Inspections of the schlieren photographs indicate a lean upward propagation limit of 12% mixture D.

For mixture E, F, and G, we performed tests only with the mixing fan on (turbulent conditions). Combustion peak pressure results of these tests indicate lean flammability limits, at which, without a mixing fan, only upward propagation flames could be observed. For mixture E, 40% H₂, 40% N₂O, and 20% CH₄, this limit occurred between 7 and 8%. The lean limit of mixture F, 35% H₂, 35% N₂O, 20% NH₃, and 10% CH₄, was observed between 8.5 and 9%. Mixture G, 29% H₂, 24% N₂O, 11% NH₃, 1% CH₄, and 35% N₂, the only mixture with nitrogen dilution, showed a lean flammability limit between 13 and 14%. 100% of mixture E or F were also flammable without air, which means, nitrous oxide was the only oxygen source. This could not be observed for mixture G, whereas 90% mixture G and 10% air was flammable.

Ignition Energies

It is known that the minimum ignition energy is a strong function of composition near the flammability limit [39]. The minimum value of ignition energy for hydrocarbon fuels in air occurs for slightly rich mixtures and is typically on the order of 0.2-0.25 mJ [39]. Near the limits, a steep rise in minimum ignition energy is observed, with mixtures outside the flammability limit exhibiting inert behavior even for very large amounts of energy. Note, that our experiments were carried out at an initial temperature of about 22°C.

Initial temperature as well as ignition energy can also show a strong influence on the flammability limits [18].

In our study, we varied the ignition energy between 40 mJ and 8 J. 40 mJ ignition energy were provided by a 30 kV pulse (low current) from an EG&G TM-11A power supply (see section Apparatus). By using a 0.5 μF capacitor charged by a Hipotronics power supply (0 - 15 kV), the spark ignition energy was increased by increasing the charging voltage (see Fig. 3). The spark was triggered (by the 30 kV, low current pulse) when the desired charging voltage was reached and stabilized. The spark ignition energy was assumed to be equal to the stored energy in the capacitor, and was therefore estimated using the relation:

$$E = \frac{1}{2} C V^2 \quad , \quad (2)$$

where E is the spark energy, C the capacitance, and V the charging voltage. The residual energy remaining in the capacitor after the discharge is less than 1% and is neglected. The actual energy deposited by spark in the gas is smaller than the stored energy [40] due to various loss mechanisms. However, due to the difficulty of directly measuring the energy, it is standard procedure to report the value given in Equ. 2 as the ignition energy [23, 41].

Methane–Nitrous Oxide Mixtures

We determined bounds on the ignition energy by carrying out a series of tests with ignition energies of 0.04, 0.2, 1.0, 2.0, 5.0 and 8.0 J. For each ignition energy, the minimum amount of methane for flammability of a methane–nitrous oxide mixture at 100 kPa initial pressure and 295 K initial temperature (no nitrogen dilution, fan on: turbulent conditions) was determined.

The measured combustion peak pressures of these runs are plotted in Fig. 14. Also shown in this plot are calculated peak pressures. A standard approach for such calculations is to use constant volume explosion estimates (AICC - adiabatic, isochoric, complete combustion) based on chemical equilibrium computations [26]. At the leanest flammable concentration (2.7% CH_4), the peak pressure is about 12 bar, close to the value obtained from N_2O decomposition alone (11.8 bar). This behavior is similar to that observed for H_2 - N_2O mixtures by Cashdollar et al. [32], who found that with sufficient ignitor energy (5000 J), hydrogen-nitrous oxide mixtures with as little as 1% H_2 could be ignited. Their limiting fuel concentration with a 58 J spark was about 6% H_2 for downward propagation. Hertzberg and Zlochower [42] propose that H-atoms catalyze N_2O decomposition and compounds such as H_2 , CH_4 and NH_3 will, in small amounts (1-2%), accelerate the decomposition reaction sufficiently to stabilize the propagation of a decomposition flame. Substantial N_2O decomposition and associated high pressures have been observed for H_2 , CH_4 and NH_3 , the last being discussed by Jones and Kerr [43]. Note that pressures are really not “high” but simply close to the 12 bar value that results from N_2O decomposition. These values seemed high to previous investigators who were used to modest

pressures for near-limit combustion of hydrocarbon-air mixtures. It was common practice (and still is) to investigate flammability limits in hydrocarbon-air mixtures with a glass apparatus. The destruction of these experiments when investigating N_2O alarmed these investigators but in hindsight it is a natural consequence of working with large amounts of N_2O . Figure 14 shows that for ignition energies above 1.0 J, the flammability limit is almost independent of the ignition energy. Increasing the ignition energy from 40 mJ to 8 J reduces the lean flammability limit from 4.8 to 2.7% CH_4 . Similar reductions in the LFL of H_2 have been obtained in H_2 - N_2O -air mixtures by Cashdollar et al. [32]. However, experiments using pyrotechnic ignitors [32] and H_2 - N_2O mixtures have shown that if the ignitor energy content is increased by several orders of magnitude (up to 5,000-10,000 J), then decomposition flames can be produced [42] even in the absence of any fuel!

Fig. 14

Ammonia–Nitrous Oxide(–Nitrogen) Mixtures

The dependence of the flammability limits on ignition energy were determined for NH_3 - N_2O and NH_3 - N_2O - N_2 mixtures for energies between 0.04 and 8 J at 100 kPa initial pressure and 295 K initial temperature (fan on: turbulent conditions). The measured combustion peak pressures of lean and rich ammonia-nitrous oxide mixtures are shown in Fig. 15 and in Fig. 16, respectively. The dependence of the flammability limits on ignition energy is much more pronounced for NH_3 - N_2O mixtures than for CH_4 - N_2O mixtures. Using 8 J ignition energy, mixtures with an initial amount of ammonia between 5.3 and 67.5% are flammable. Decreasing the ignition energy from 8.0 to 0.1 J narrows the flammable region to 7.5 - 63.0% NH_3 . With 0.04 J ignition energy, 11.5 - 54.0% NH_3 are required for flammability. Calcote et al. [41] measured a minimum spark ignition energy of 0.07 mJ for a stoichiometric NH_3 - N_2O mixture (40% NH_3 , 60% N_2O) at atmospheric pressure. Our measured ignition energy bounds at 54% nitrogen dilution are shown in Fig. 17. In addition, we performed some tests with ammonia–air mixtures. A stoichiometric ammonia–air mixture at 100 kPa initial pressure (21.9% ammonia, 78.1% air) could not be ignited with energies less than 50 mJ, whereas the mixture was flammable for spark ignition energies above 100 mJ. Buckley and Husa [36] obtained a minimum ignition energy of 680 mJ for ammonia–air mixtures.

Fig. 15

Fig. 16

Fig. 17

Hydrogen–Methane–Ammonia–Nitrous Oxide–Oxygen–Nitrogen Mixtures

We performed further ignition energy tests with three different hydrogen–methane–ammonia–nitrous oxide–nitrogen mixtures (see mixtures E, F, and G in Table 2) in air. The initial conditions were: $p_0 = 100$ kPa, $T_0 = 295$ K, and fan on (turbulent conditions). The ignition energy was again varied between 40 mJ and 8 J.

For mixtures E and G we observed almost no variation of the lean flammability limit in air by decreasing the ignition energy from 8 to 0.04 J, whereas for mixture F the lean limit increased about 0.5%, from 8.5 - 9% to 9 - 9.5%.

Flame Speeds

When predicting the combustion behavior of multiple component mixtures, the flame speed of the pure mixtures in oxidizer can give some insight into deviation from ideal behavior. For example, when H_2 is mixed with CH_4 and burned in air, the difference in flame speeds causes CH_4 to act as a diluent for some stoichiometries. Flame speeds near the lean limit for these fuels are not very well known. Flame speed measurements provide a method of comparing very lean mixtures. Ronney [44] performed flame speed measurements for lean NH_3 -air mixtures in microgravity. The method used by Ronney to calculate burning velocities in closed vessel experiments is described in Andrews and Bradley [45].

In the idealized flame propagation experiment (such as the “soap bubble” technique [45]), the pressure initially remains constant during combustion and the flame front is spherical. The flame front expands radially, and it is assumed that the burned gas inside the flame ball remains stationary. Therefore, the laminar burning velocity is the difference between the expansion rate of the flame front, V_f , and the velocity of the unburned reactants. The laminar burning velocity S_L^0 is therefore

$$S_L^0 = V_f - u. \quad (3)$$

The continuity equation may be applied to obtain a relation between the burning velocity and the expansion rate of the bubble.

$$\rho_u S_L^0 = \rho_b V_f, \quad (4)$$

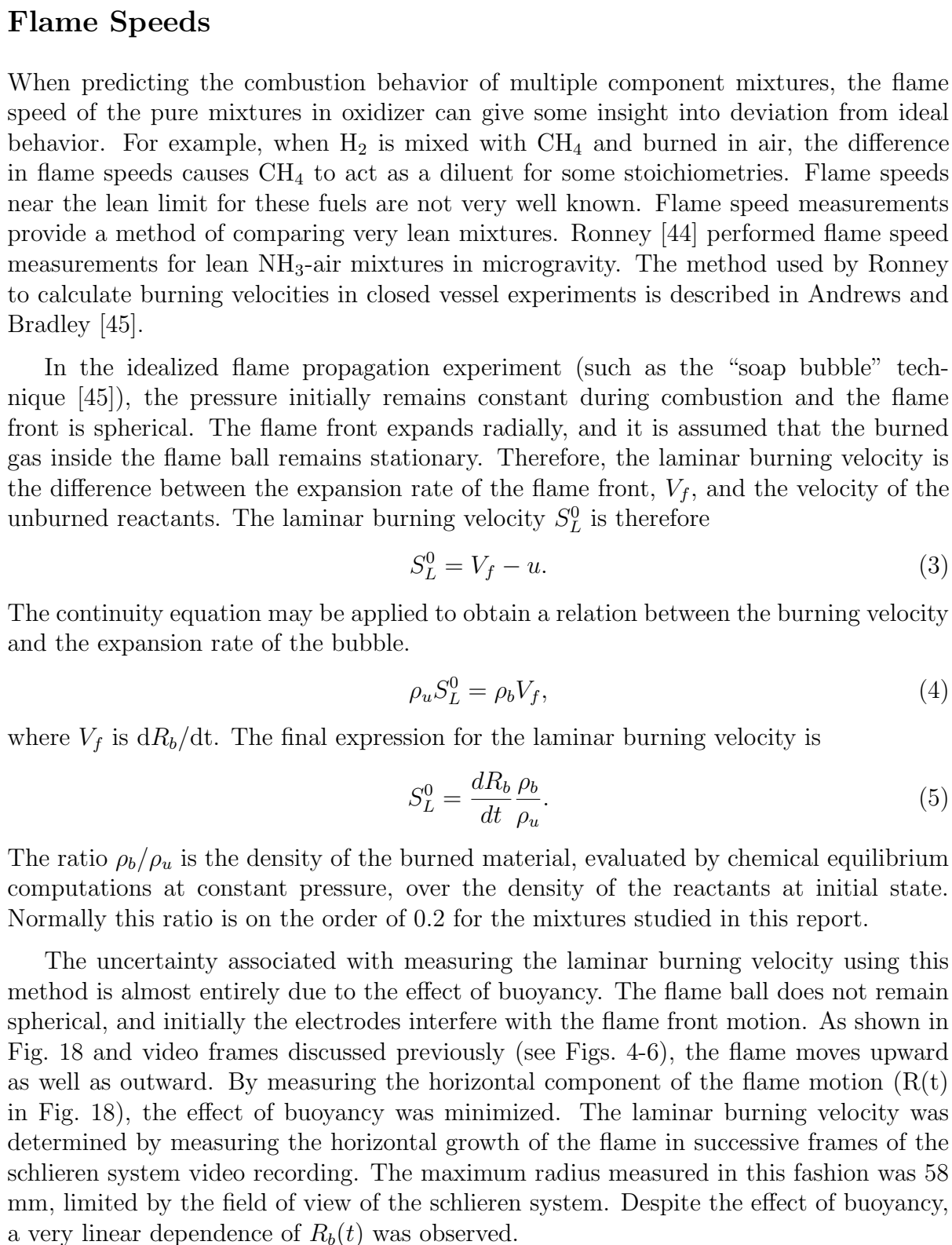
where V_f is dR_b/dt . The final expression for the laminar burning velocity is

$$S_L^0 = \frac{dR_b}{dt} \frac{\rho_b}{\rho_u}. \quad (5)$$

The ratio ρ_b/ρ_u is the density of the burned material, evaluated by chemical equilibrium computations at constant pressure, over the density of the reactants at initial state. Normally this ratio is on the order of 0.2 for the mixtures studied in this report.

The uncertainty associated with measuring the laminar burning velocity using this method is almost entirely due to the effect of buoyancy. The flame ball does not remain spherical, and initially the electrodes interfere with the flame front motion. As shown in Fig. 18 and video frames discussed previously (see Figs. 4-6), the flame moves upward as well as outward. By measuring the horizontal component of the flame motion ($R(t)$ in Fig. 18), the effect of buoyancy was minimized. The laminar burning velocity was determined by measuring the horizontal growth of the flame in successive frames of the schlieren system video recording. The maximum radius measured in this fashion was 58 mm, limited by the field of view of the schlieren system. Despite the effect of buoyancy, a very linear dependence of $R_b(t)$ was observed.

The two lines shown in Fig. 18 were obtained by drawing lines through the (x,y) coordinates of largest horizontal extent of each flame. In practice, the coordinates were


 Fig. 18

not perfectly aligned and so a fit to the data points was required. The growth data was fit to a linear function $R_b(t) = at + b$ and the slope was interpreted as the flame speed V_f . The slope can be determined quite accurately (the standard error is typically less than 5%) and the uncertainty in the flame speed is almost entirely due to unquantified effects of buoyancy. Comparisons with microgravity, two-kernel and LDV [46] measurements are quite favorable.

Subsequent work by O. Kunz ([47]) has shown that this technique is in reasonable agreement with other more accepted methods such as the t^3 analysis of the pressure traces for slow flames. Other work by K.S. Raman [46] on LDV measurement of very slow flames indicate that the simple maximum width approach is reasonable for very lean H_2 flames even though the flames are highly distorted by buoyancy.

In Fig. 4 the apparent drift to the left is an optical illusion caused by the fact that the ignition point is not in the center of the chamber. In all cases, such offsets were eliminated by finding the largest width of the flame and then dividing by 2 to obtain effective radius.

Ammonia–Air–Nitrous Oxide Mixtures

NH_3 -air- N_2O tests were conducted over the range of 12-24% NH_3 . Three N_2O concentrations were used, 0, 4, and 8%. All of these tests were carried out at initial conditions of 100 kPa and 295 K with the mixing fan off (quiescent conditions). The results indicate that the downward propagation limit of NH_3 -air mixtures is decreased as N_2O is added to the mixture. Addition of N_2O resulted in a significant increase in the peak pressures for a given NH_3 concentration. The downward propagation limit decreased from 18 to 15% NH_3 with the addition of 8% N_2O .

Laminar burning velocity and density ratio (ρ_u/ρ_b) both increase with increasing flame temperature (increasing N_2O addition). This results in a higher value of apparent flame speed, dR/dt , and enhanced propagation. The laminar burning velocities are summarized in Fig. 19. The addition of the N_2O appears to increase the laminar burning velocity by a factor of 2 with the 8% N_2O from the NH_3 -air case. A comparison between Ronney's study of NH_3 -air flames in microgravity [44] and our investigation shows that our values of the laminar burning velocities are within ± 1 cm/s of Ronney's results (see Fig. 19). Although the absolute error is reasonable, since near-limit burning speeds are less than 5 cm/s, the percentage error can be high. The very low burning speeds near the limiting concentration indicate that buoyancy will have a significant effect on flame propagation which could account for the differences between the present results and those of Ronney.

Fig. 19

Hydrogen–Methane–Ammonia–Nitrous Oxide–Oxygen–Nitrogen Mixtures

Laminar burning velocities were measured for mixtures A - G (see Table 2) in air at quiescent conditions, which means, the mixing fan was turned off and the gas allowed to

come to rest prior to ignition. All tests were carried out at initial conditions of 100 kPa and 295 K. The initial amounts of mixtures A - G were varied between 7 and 22%. The results are shown in Fig. 20.

The solid circles in Fig. 20 show the laminar burning velocities of mixture A as a function of concentration. A burning velocity of 6 cm/s was measured at the downward propagation limit of 15%. At the upward propagation limit of 7% we obtained a laminar burning velocity of 1.7 cm/s. For mixture B, the laminar burning velocity corresponding to the downward propagation limit near 15% is about 4.8 cm/s. For 8% mixture B in air, we measured a laminar burning velocity of 1.75 cm/s. The laminar burning velocity of mixture C is 5.4 cm/s at the downward propagation limit close to 16% and 1.8 cm/s for 9% mixture C. The laminar burning velocity measured for mixture D is 5.3 cm/s at the downward propagation limit of 20% and 1.9 cm/s for 11% mixture D. For mixture G we measured just one laminar burning velocity at 17.5%. The result is close to what was obtained for mixture D. The laminar burning velocities of mixture E and mixture F in air seem to be of the same order than what was obtained for mixture A - D for concentrations of less than 10%, whereas the increase of the laminar burning velocity with increasing concentration is much higher.

Fig. 20

4 Conclusions

The present study focuses on combustion characteristics of fuel-nitrous oxide mixtures. The fuels investigated are hydrogen, methane and ammonia as well as several hydrogen-methane-ammonia mixtures. Flammability limits, ignition energies, and flame speeds have been measured. Experiments were carried out in a 11.25- and a 400-liter combustion vessel at initial pressures and temperatures of 100 kPa and 295 K, respectively.

Flammability maps of hydrogen-nitrous oxide-nitrogen, methane-nitrous oxide-nitrogen, ammonia-nitrous oxide-nitrogen, and of ammonia-nitrous oxide-air were determined using a spark ignition energy of 8 J. The mixing fan was running during combustion (turbulent conditions). The results are presented in Table 3. The influence of small amounts of oxygen (< 5%) on the flammability of methane-nitrous oxide-nitrogen mixtures has been investigated. No pronounced dependence of the flammability limits on 3 - 5% oxygen could be observed.

Ignition energy bounds of methane-nitrous oxide, ammonia-nitrous oxide, and ammonia-nitrous oxide-nitrogen mixtures have been determined. The behavior of lean fuel-N₂O mixtures can be divided into two regimes: 1) low-to-moderate ignition energy (up to 10 J); 2) high ignition energy (above 5000 J). For the low-to-moderate energy regime, there is a well-defined minimum concentration of fuel (LFL) independent of ignition energy up to some value, at least 10 J. For the high-energy regime, N₂O decomposition reactions can be initiated irrespective of the amount of fuel as long as the energy is released rapidly enough. The precise details of the chemical and physical mechanism

Fuel	LFL [% Fuel]	UFL [% Fuel]	Inert [%]
H ₂	4.5~5.0	76~80	N ₂ : 76
CH ₄	2.5~3.0	43~50	N ₂ : 70.5
NH ₃	5.0~5.2	67.5~68	N ₂ : 61
NH ₃	"	"	air: 85

Table 3: Flammability limits for fuel-N₂O mixtures at $p_0 = 100$ kPa and $T_0 = 295$ kPa, 8 J ignition energy and mixing fan on (turbulent conditions).

are not well understood at present but for the purposes of most safety assessments, it is probably sufficient to characterize the behavior in the low-to-moderate energy regime. It remains an intriguing problem in combustion science to determine the details of the flame initiation and propagation in very lean fuel-nitrous oxide mixtures.

Flame speeds have been measured and laminar burning velocities have been determined for ammonia-air-nitrous oxide and various hydrogen-methane-ammonia-nitrous oxide-oxygen-nitrogen mixtures. Generally speaking, increasing the initial amount of nitrous oxide in flammable gases increases the laminar burning velocity clearly as soon as the combustion temperature is sufficiently high (> 1200 K).

Acknowledgments

This work was supported by the U.S. Department of Energy under contract 929Q0015-3A, DOE W-7405-ENG-36. We thank Jerry Johnson for the support.

References

- [1] Sullivan L. H. et al. A safety assessment for proposed pump mixing operations to mitigate episodic gas releases in tank 241-SY-101: Hanford Site, Richland, Washington, Revision 14. Los Alamos National Laboratory Report LA-UR-92-3196, April 1995.
- [2] ASTM D56. *Standard Test Method for Flash Point by Tag Closed Tester*. American Society for Testing and Materials, 1988.
- [3] ASTM E582. *Standard Test Method for Minimum Ignition Energy and Quenching Distance in Gaseous Mixtures*. American Society for Testing and Materials, 1988.
- [4] ASTM E1232. *Standard Test Method for Temperature Limit of Flammability of Chemicals*. American Society for Testing and Materials, 1991.
- [5] ASTM E681. *Standard Test Method for Concentration Limits of Flammability of Chemicals*. American Society for Testing and Materials, 1985.
- [6] H. F. Coward and G. W. Jones. Limits of flammability of gases and vapors. Bulletin 503, Bureau of Mines, 1952.
- [7] M. G. Zabetakis. Flammability characteristics of combustible gases and vapors. Bulletin 627, Bureau of Mines, 1965.
- [8] M.G. Zabetakis, G. S. Scott, and G. W. Jones. Limits of flammability of paraffin hydrocarbons in air. *Ind. Eng. Chem.*, 43(9):2120–2124, 1951.
- [9] J. E. Shepherd, J. J. Lee, and J. C. Krok. Spark ignition measurements in Jet A. Explosion Dynamics Laboratory Report FM97-9, California Institute of Technology, June 1998.
- [10] J. J. Lee and J. E. Shepherd. Spark Ignition Measurements in Jet A: part II. Explosion Dynamics Laboratory Report FM99-7, California Institute of Technology, December 1999.
- [11] D. B. Spalding. A theory of inflammability limits and flame quenching. *Proc. Roy. Soc. (London), Series A*, 240:83, 1957.
- [12] C. K. Law and F. N. Egolfopoulos. A unified chain-thermal theory of fundamental flammability limits. In *Twenty-Fourth Symp. (Intl) Combustion*, pages 137–144, Pittsburgh, PA, 1992. The Combustion Institute.
- [13] C. J. Sung and C. K. Law. Extinction mechanisms of near-limit premixed flames and extended limits of flammability. In *Twenty-Sixth Symp. (Intl) Combustion*, pages 865–873, Pittsburgh, PA, 1992. The Combustion Institute.

- [14] M. N. Bui-Pham, A. E. Lutz, J. A. Miller, M. Desjardin, D. M. O'Shaughnessaey, and R. J. Zondlak. Rich flammability limits in $\text{ch}_3\text{oh}/\text{co}/\text{diluent}$ mixtures. *Combust. Sci. Tech.*, 109:71–91, 1995.
- [15] W. D. Breshears. Falloff behavior in the thermal dissociation rate of N_2O . *Journal of Physical Chemistry*, 99:12529 – 12535, 1995.
- [16] U. J. Pfahl, J. E. Shepherd, and W. D. Breshears. Nitrous oxide consumption during combustion of hydrogen–methane–ammonia–nitrous oxide–air mixtures. *Combustion and Flame*, in press, 1998.
- [17] H. Le Chatelier and O. Boudouard. Limits of flammability of combustible vapors. *Compt. Rend.*, 126:1510, 1898.
- [18] M. G. Zabetakis. Flammability characteristics of combustible gases and vapors. Bulletin 627, Bureau of Mines, 1965.
- [19] M. C. Ross and J. E. Shepherd. Lean combustion characteristics of hydrogen-nitrous oxide-ammonia mixtures in air. Part I. Explosion Dynamics Laboratory Report FM96-4, California Institute of Technology, Pasadena, CA, July 1996.
- [20] P. D. Ronney. Effect of gravity on laminar premixed gas combustion II: ignition and extinction phenomena. *Combustion and Flame*, 62:121–133, 1985.
- [21] K.-G. Strid. Experimental techniques for the determination of ignition energy. In *Oxidation and Combustion Reviews*, pages 1–46, 1973.
- [22] H. F. Coward and G. W. Jones. Limits of flammability of gases and vapors. Bulletin 503, Bureau of Mines, 1952.
- [23] B. Lewis and G. Von Elbe. Combustion, flames, and explosions of gases. *Academic Press, Inc., New York*, 1961.
- [24] M. Hertzberg. The theory of flammability limits, natural convection. Bulletin 8127, Bureau of Mines, 1976.
- [25] A. Abbud-Madrid and P. D. Ronney. Effects of radiative and diffusive transport processes on premixed flames near flammability limits. In *Twenty-Third Symp. (Intl) Combustion*, pages 423–431, Pittsburgh, PA, 1990. The Combustion Institute.
- [26] W. C. Reynolds. *The Element Potential Method for Chemical Equilibrium Analysis: Implementation in the Interactive Program STANJAN*. Stanford University, Dept. of Mechanical Engineering, Stanford, CA, 3rd edition, January 1986.
- [27] S. Smith and J. W. Linnett. The upper limits of inflammability of hydrogen–air and hydrogen–nitrous oxide mixtures. *J. Chem. Soc. (London)*, Part I:37–43, 1953.

- [28] K. Posthumus. On explosion regions of gas mixtures, in which one or two of the gases are endothermic. *Rec. trav. chim.*, 49:309–347, 1930.
- [29] M. J. van der Wal. Explosive and nonexplosive reactions between nitrogen oxides and flammable gases. *Rec. trav. chim.*, 53:97–117, 1934.
- [30] F. E. Scott, R. W. Van Dolah, and M. G. Zabetakis. The flammability characteristics of the system $\text{H}_2\text{-NO-N}_2\text{O-air}$. In *Sixth Symp. (Intl) Combustion*, pages 540–545, Pittsburgh, PA, 1957. The Combustion Institute.
- [31] Yu. N. Shebeko, S. G. Tsarichenko, A. Ya. Korolchenko, A. V. Trunev, V. Yu. Navzenya, S. N. Papkov, and A. A. Zaitzev. Burning velocities and flammability limits of gaseous mixtures at elevated temperatures and pressures. *Combustion and Flame*, 102:427–437, 1995.
- [32] K.L. Cashdollar, M. Hertzberg, I.A. Zlochower, C.E. Lucci, G. M. Green, and R. A. Thomas. Laboratory flammability studies of mixtures of hydrogen, nitrous oxide, and air. Final Report WHC-SD-WM-ES-219, Bureau of Mines, June 1992.
- [33] D. L. Fenton, A. S. Khan, R. D. Kelley, and K. S. Chapman. Combustion characteristics review of ammonia–air mixtures. *ASHRAE Transactions*, 3922:1–10, 1995.
- [34] J. W. Armitage and P. Gray. Flame speeds and flammability limits in the combustion of ammonia: ternary mixtures with hydrogen, nitric oxide, nitrous oxide or oxygen. *Combustion and Flame*, 9:173–184, 1965.
- [35] D. G. R. Andrews and P. Gray. Combustion of ammonia supported by oxygen, nitrous oxide or nitric oxide: laminar flame propagation at low pressures in binary mixtures. *Combustion and Flame*, 8:113–126, 1964.
- [36] W. L. Buckley and H. W. Husa. Combustion properties of ammonia. *Chemical Engineering Progress*, 58, 2:81–84, 1962.
- [37] W. P. Jorissen and B. L. Ongkiehong. The explosion regions of hydrogen–ammonia–air and hydrogen–ammonia–oxygen mixtures. *Rec. trav. chim.*, 45:224–231, 1926.
- [38] A. G. White. Limits for the propagation of flame at various temperatures in mixtures of ammonia with air and oxygen. *J. Chem. Soc.*, 121:1688–1695, 1922.
- [39] J.M. Kuchta. Investigation of fire and explosion accidents in the chemical, mining, and fuel-related industries—a manual. Bulletin 680, U.S. Bureau of Mines, 1985.
- [40] K.-G. Strid. Experimental techniques for the determination of ignition energy. *Oxidation and Combustion Reviews*, pages 1–46, 1973.
- [41] H. F. Calcote, Jr. C. A. Gregory, C. M. Barnett, and Ruth B. Gilmer. Spark ignition. *Industrial and Engineering Chemistry*, 44, 11:2656–2662, 1952.

-
- [42] M. Hertzberg and I.A. Zlochower. Explosibility of nitrous oxide gas: The effect of H-atom-bearing impurities. Abstract, Joint Meeting of British and German Sections of the Combustion Institute, March 29-April 3, Cambridge, England, 1993.
- [43] E. Jones and J.C. Kerr. Inflammability limits of ammonia, nitrous oxide, and air. *J.S.C.I.*, 68:31–34, 1949.
- [44] P. D. Ronney. Effect of chemistry and transport properties on near-limit flames at microgravity. *Combustion Science and Technology*, 59:123–141, 1987.
- [45] G. E. Andrews and D. Bradley. *Combustion and Flame*, 18:133, 1972.
- [46] K. S. Raman. Laminar burning velocities of lean hydrogen-air mixtures. Explosion Dynamics Laboratory Report FM97-15, California Institute of Technology, Pasadena, CA, January 1998.
- [47] Oliver Kunz. Combustion characteristics of hydrogen- and hydrocarbon-air mixtures in closed vessels. Technical Report FM98-4, GALCIT, California Institute of Technology, March 1998.
- [48] G. W. Jones and G. St. J. Perrott. Oxygen required for the propagation of hydrogen, carbon monoxide, and methane flames. *Ind. and Eng. Chem.*, 19:985–989, 1927.

5 Figures

Figure captions:

Fig. 1: Schematic diagram of the 11.25 liter constant volume combustion vessel.

Fig. 2: Schematic diagram of the color-schlieren video-system.

Fig. 3: Schematic diagram of the spark ignition system.

Fig. 4: Sequence of video frames from experiment 180: 20 kPa NH₃, 80 kPa air; initial pressure $p_0 = 100$ kPa, initial temperature $T_0 = 22^\circ\text{C}$; fan off (quiescent conditions); combustion peak pressure = 5.1 bar.

Fig. 5: Sequence of video frames from experiment 183: 18 kPa NH₃, 82 kPa air; initial pressure $p_0 = 100$ kPa, initial temperature $T_0 = 22^\circ\text{C}$; fan on (turbulent conditions); combustion peak pressure = 6.7 bar.

Fig. 6: Sequence of video frames from experiment 159: 7 kPa H₂, 7 kPa N₂O, 6 kPa NH₃, 80 kPa air; initial pressure $p_0 = 100$ kPa, initial temperature $T_0 = 22^\circ\text{C}$; fan off (quiescent conditions); combustion peak pressure = 5.4 bar.

Fig. 7: Literature data of flammability limits of hydrogen–air–nitrogen [48], hydrogen–oxygen–nitrogen [31, 22], and hydrogen–nitrous oxide–nitrogen mixtures [28, 27, 30, 29]; initial pressure $p_0 = 1$ atm, initial temperature $T_0 = 25^\circ\text{C}$.

Fig. 8: Flammability limits of hydrogen–nitrous oxide–nitrogen mixtures; initial pressure $p_0 = 100$ kPa, initial temperature $T_0 = 22^\circ\text{C}$.

Fig. 9: Flammability limits of methane–nitrous oxide–nitrogen, methane–nitrous oxide–oxygen–nitrogen, and methane–oxygen–nitrogen mixtures (Zabetakis [18] data is only for CH₄-O₂-N₂); initial pressure $p_0 = 100$ kPa, initial temperature $T_0 = 22^\circ\text{C}$.

Fig. 10: Influence of small amounts of oxygen on the flammability limits of methane–nitrous oxide–nitrogen mixtures; initial pressure $p_0 = 100$ kPa, initial temperature $T_0 = 22^\circ\text{C}$.

Fig. 11: Flammability limits of ammonia–nitrous oxide–nitrogen mixtures; initial pressure $p_0 = 100$ kPa, initial temperature $T_0 = 22^\circ\text{C}$.

Fig. 12: Flammability limits of ammonia–nitrous oxide–air mixtures; initial pressure $p_0 = 100$ kPa, initial temperature $T_0 = 22^\circ\text{C}$.

Fig. 13: Upward and downward propagation flammability limits of hydrogen–ammonia–air mixtures; initial pressure $p_0 = 100$ kPa, initial temperature $T_0 = 22^\circ\text{C}$.

Fig. 14: Peak pressure vs. initial methane concentration for fuel–lean methane–nitrous oxide mixtures at various ignition energies.

Fig. 15: Peak pressure vs. initial ammonia concentration for fuel–lean ammonia–nitrous oxide mixtures at various ignition energies.

Fig. 16: Peak pressure vs. initial ammonia concentration for fuel–rich ammonia–nitrous oxide mixtures at various ignition energies.

Fig. 17: Peak pressure vs. initial ammonia concentration for ammonia–nitrous oxide–nitrogen mixtures at various ignition energies.

Fig. 18: Experimentally observed flame development showing a typical buoyant flame near the lean flammability limit; $R(t)$: flame radius as a function of time.

Fig. 19: Laminar burning velocity vs. initial ammonia concentration of ammonia–nitrous oxide–air mixtures; data from Ronney’s [44] microgravity experiments are also plotted.

Fig. 20: Laminar burning velocity vs. initial mixture concentration of various hydrogen–methane–ammonia–nitrous oxide–nitrogen mixtures in air.

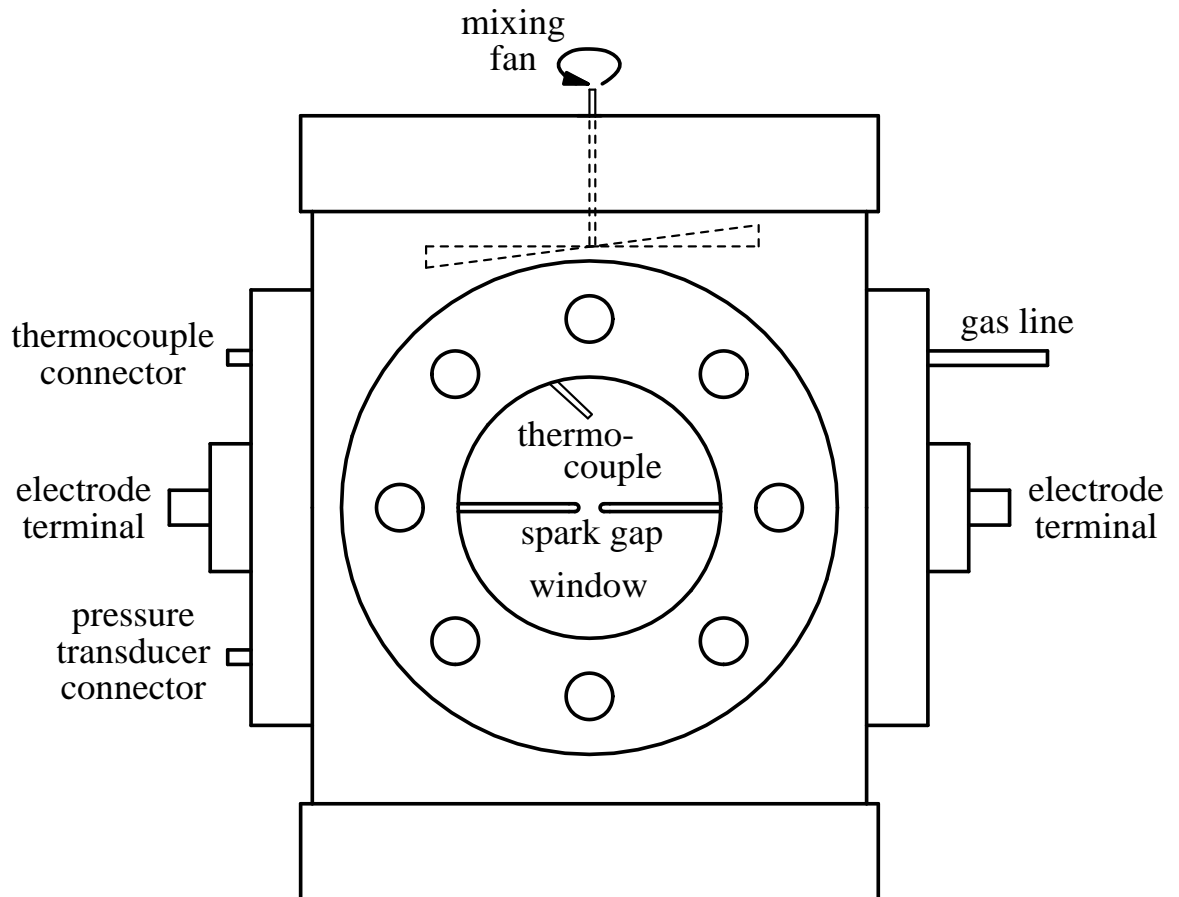


Figure 1:

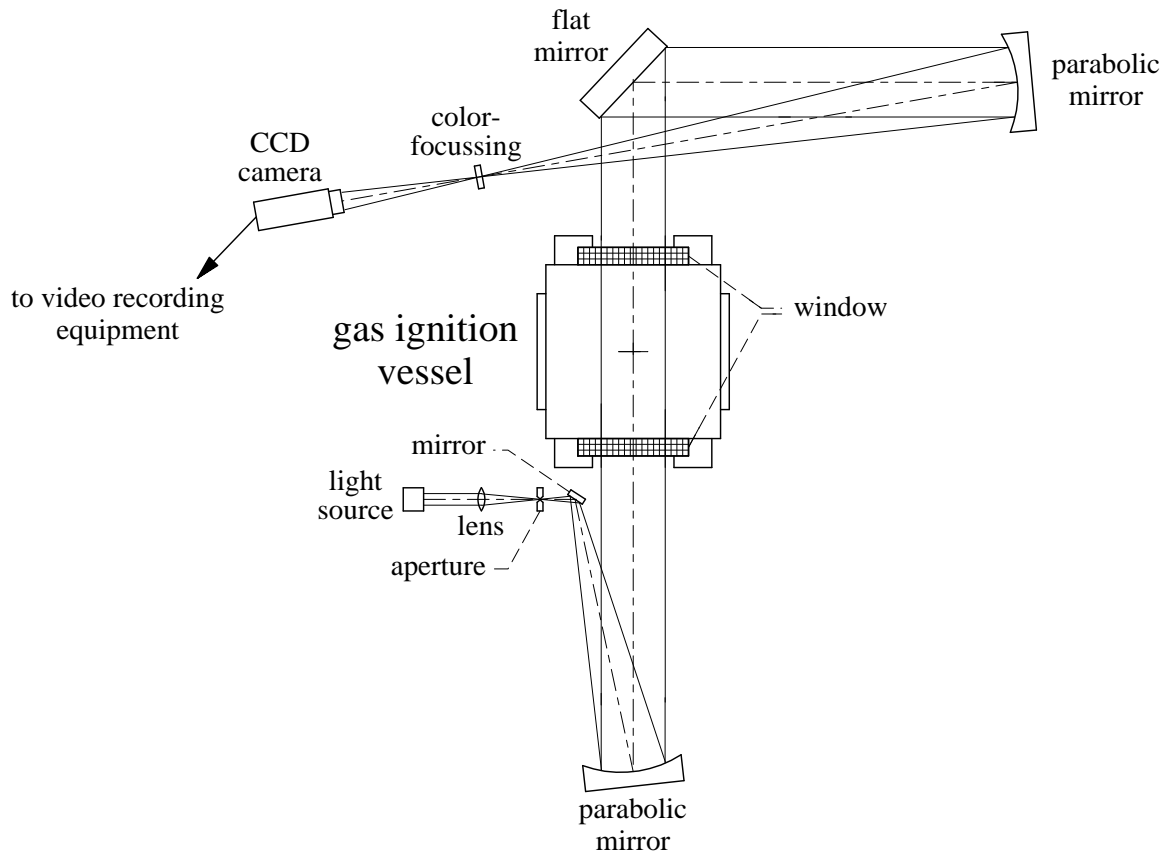


Figure 2:

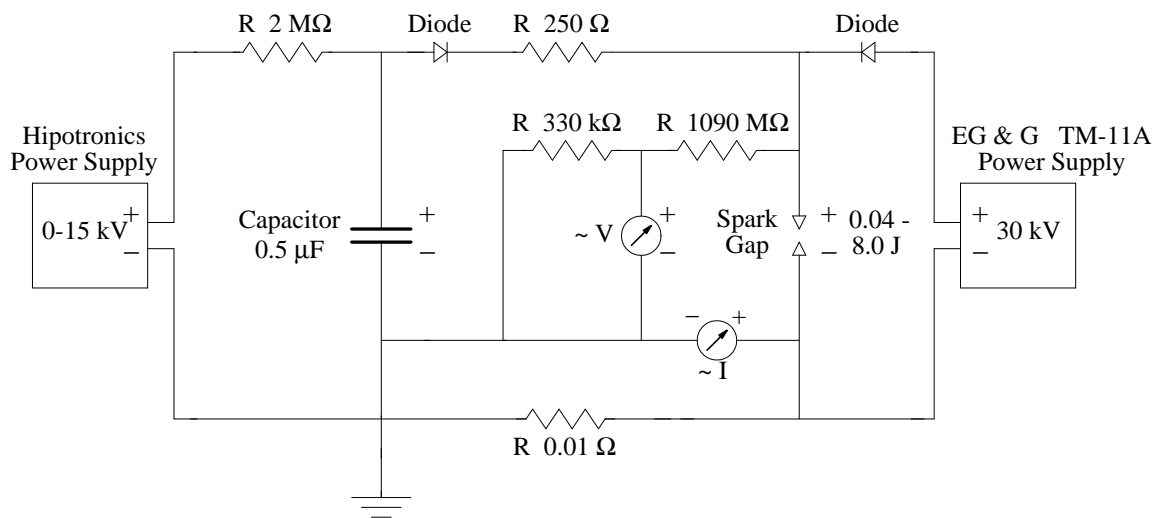


Figure 3:

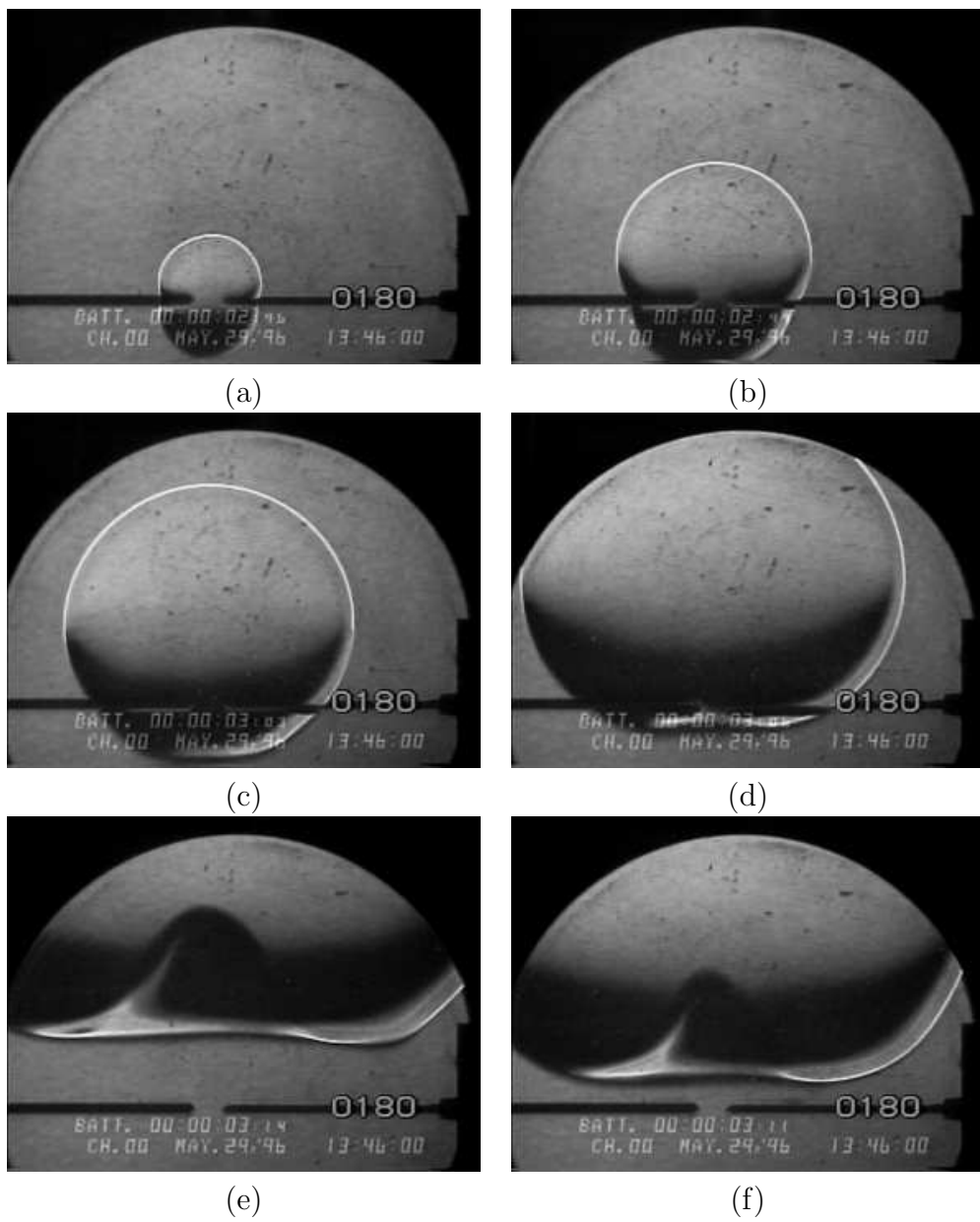


Figure 4:

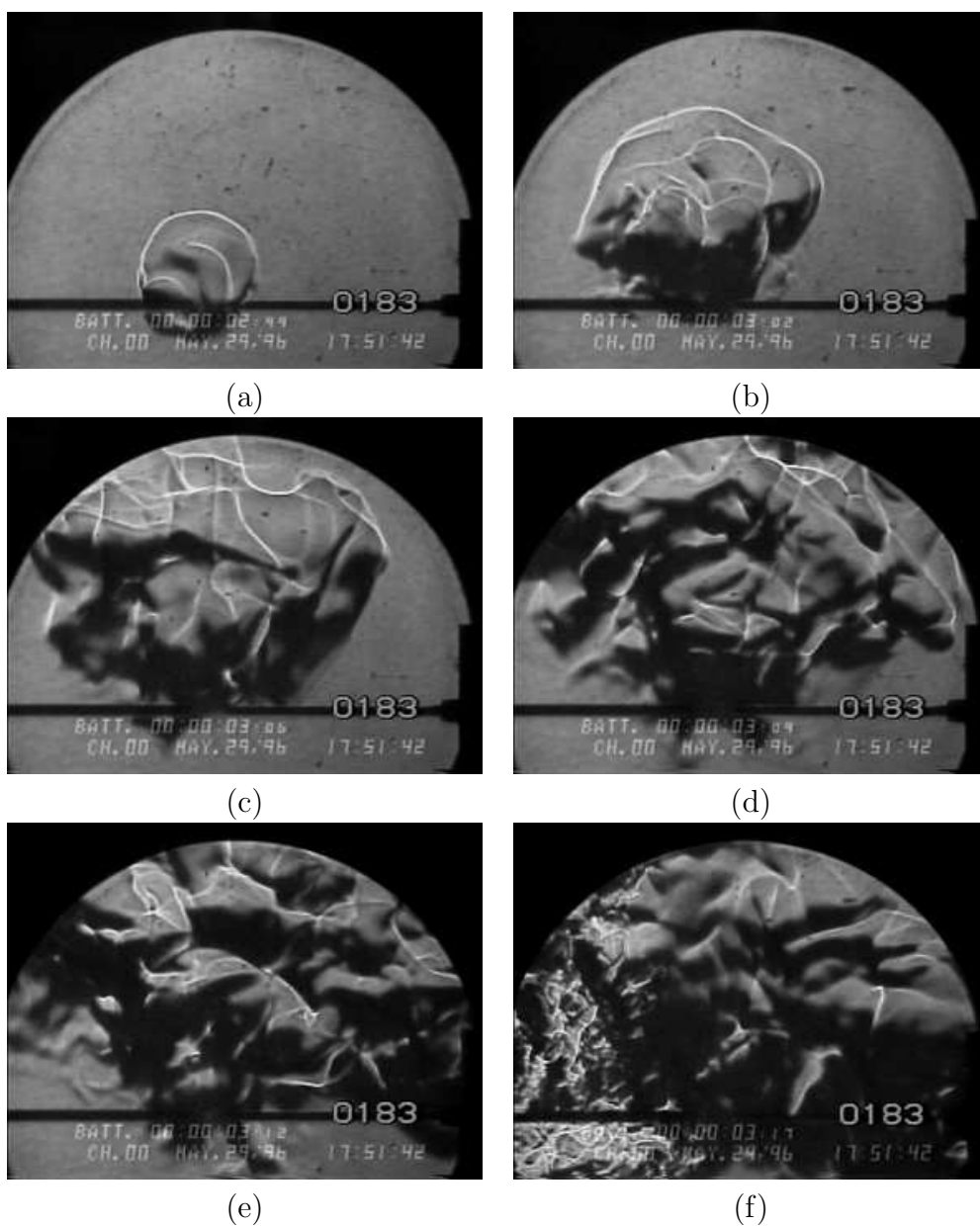


Figure 5:

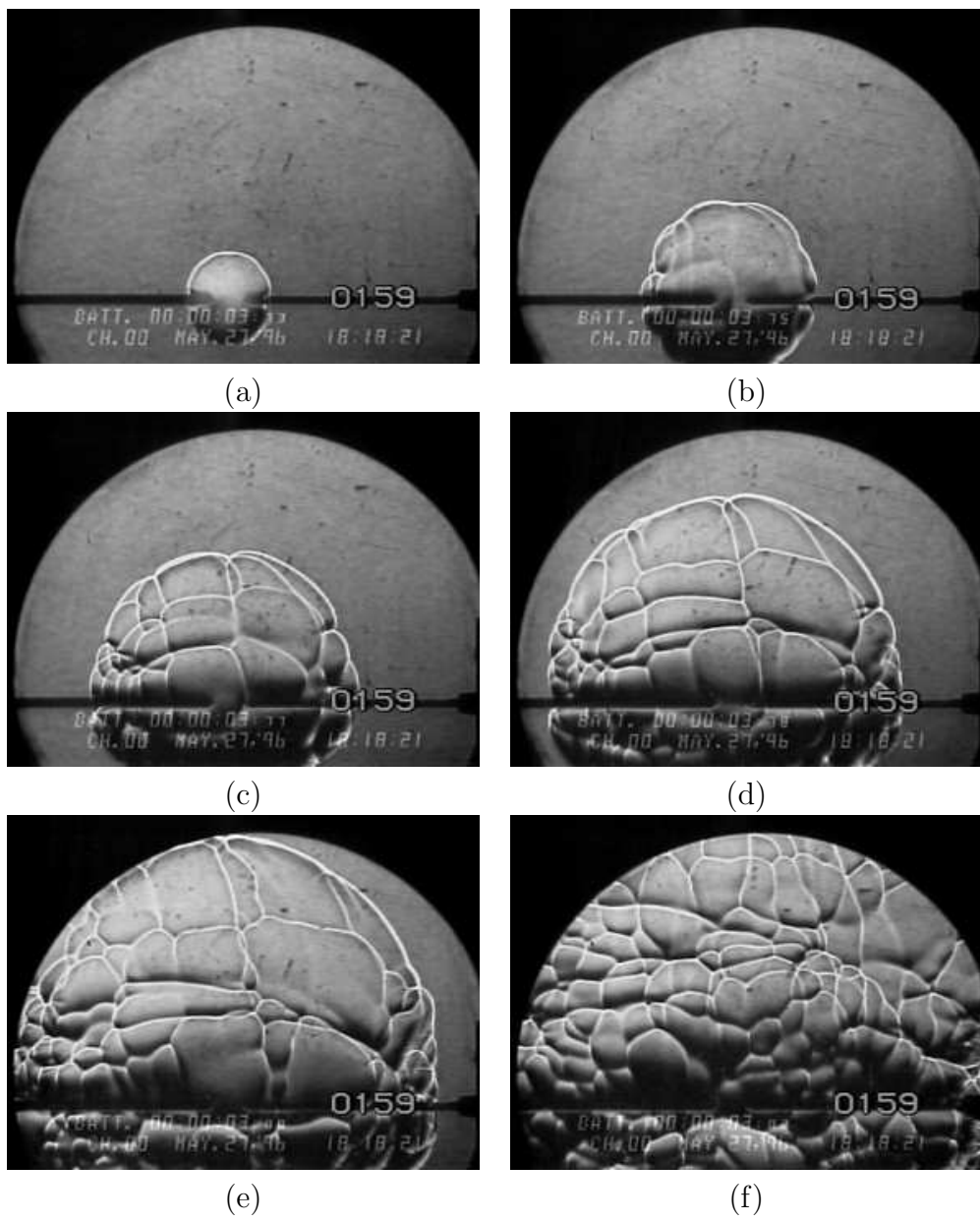


Figure 6:

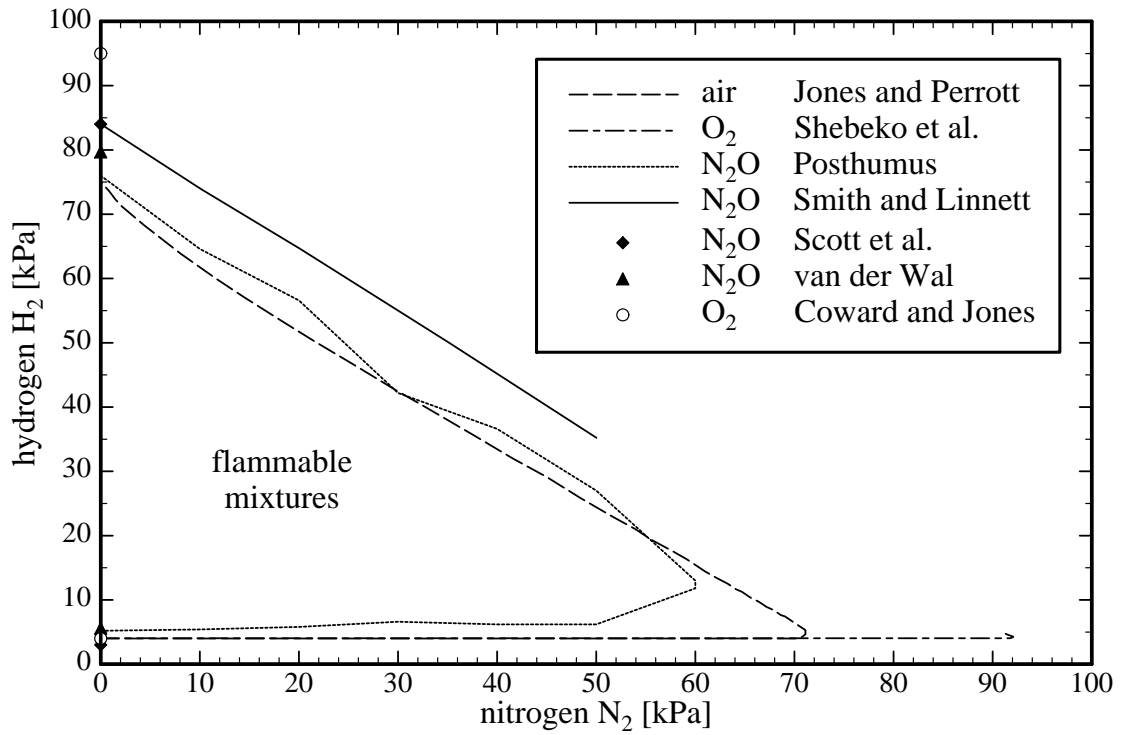


Figure 7:

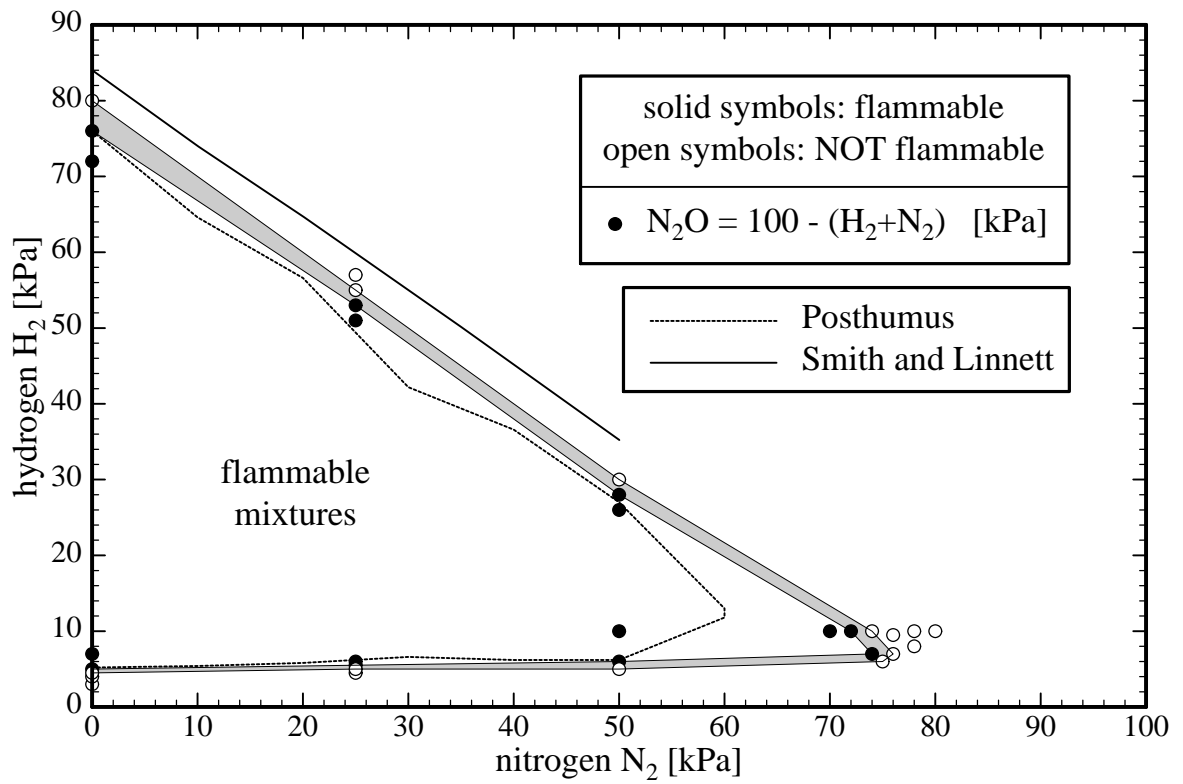


Figure 8:

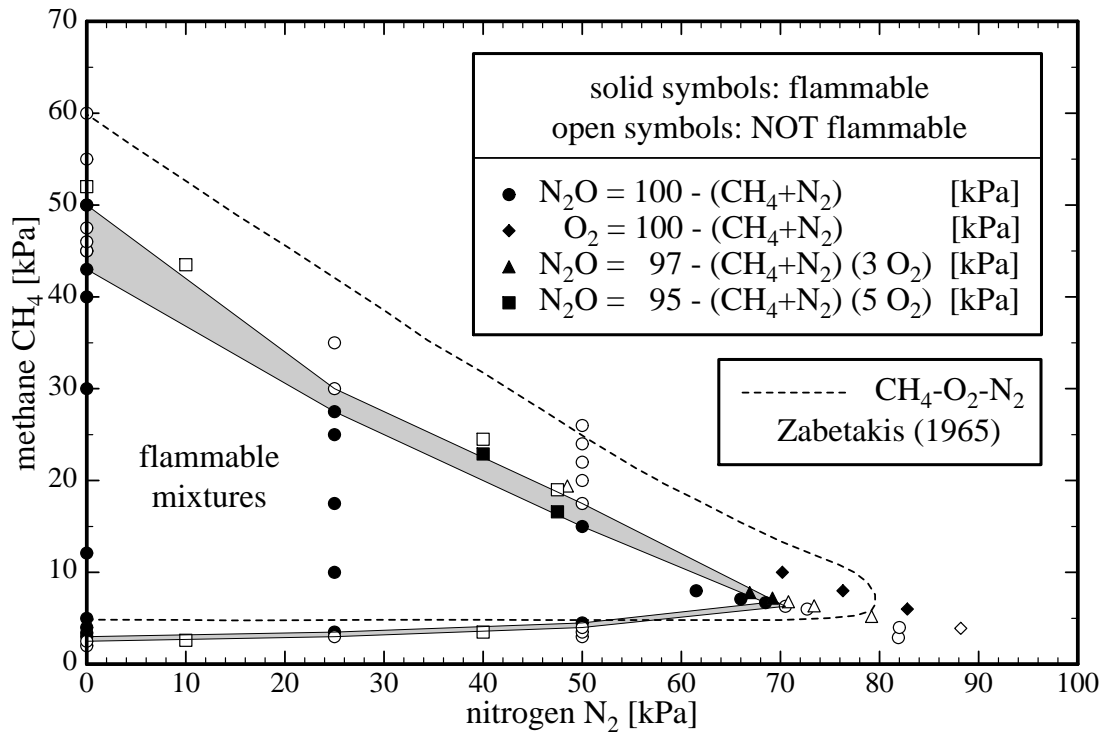


Figure 9:

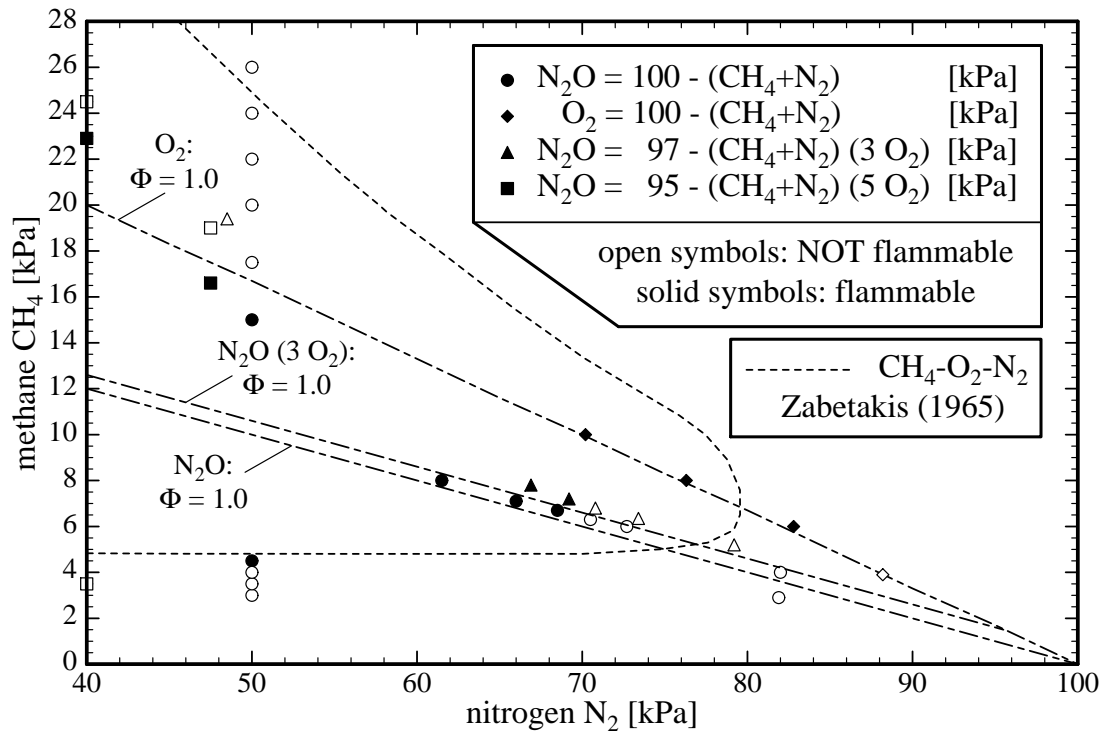


Figure 10:

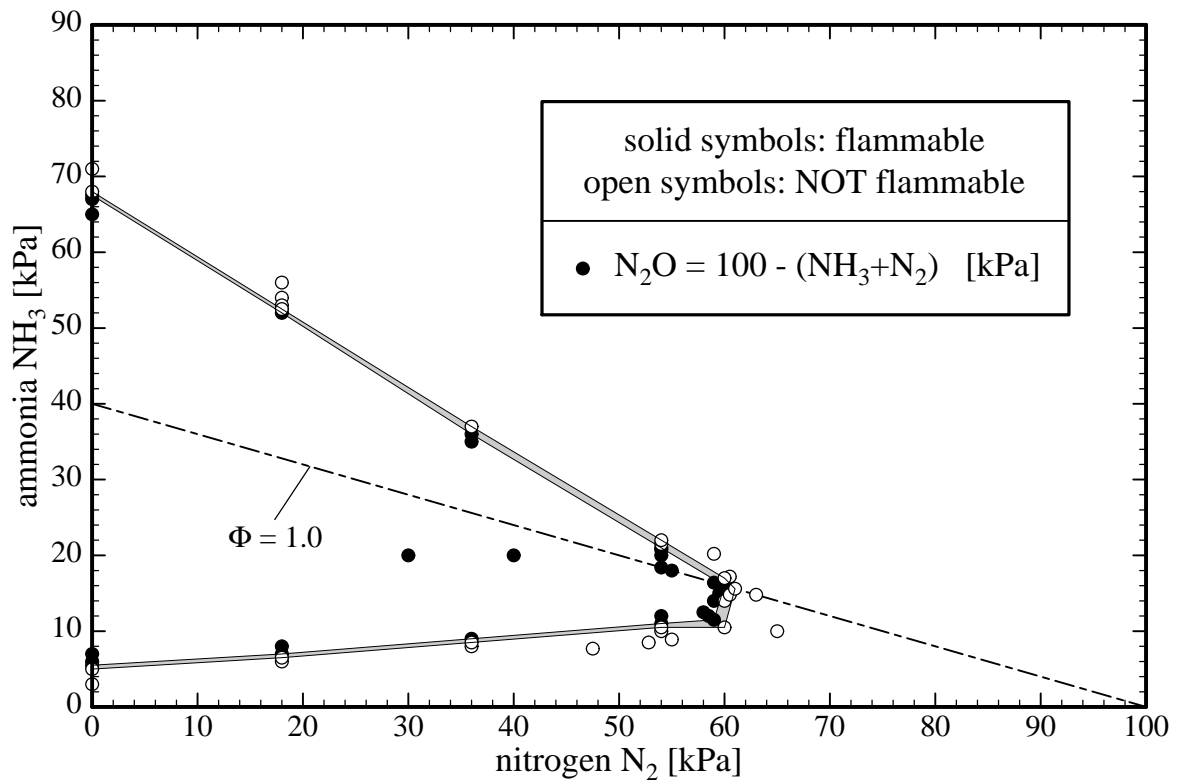


Figure 11:

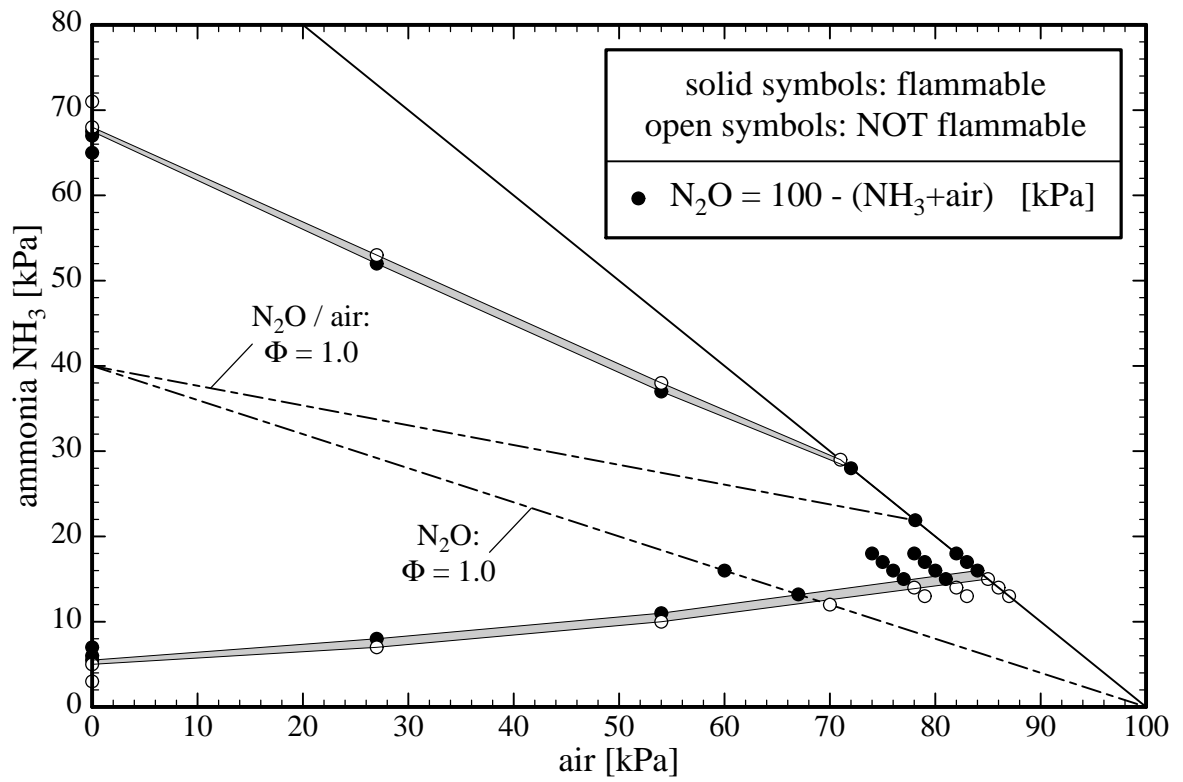


Figure 12:

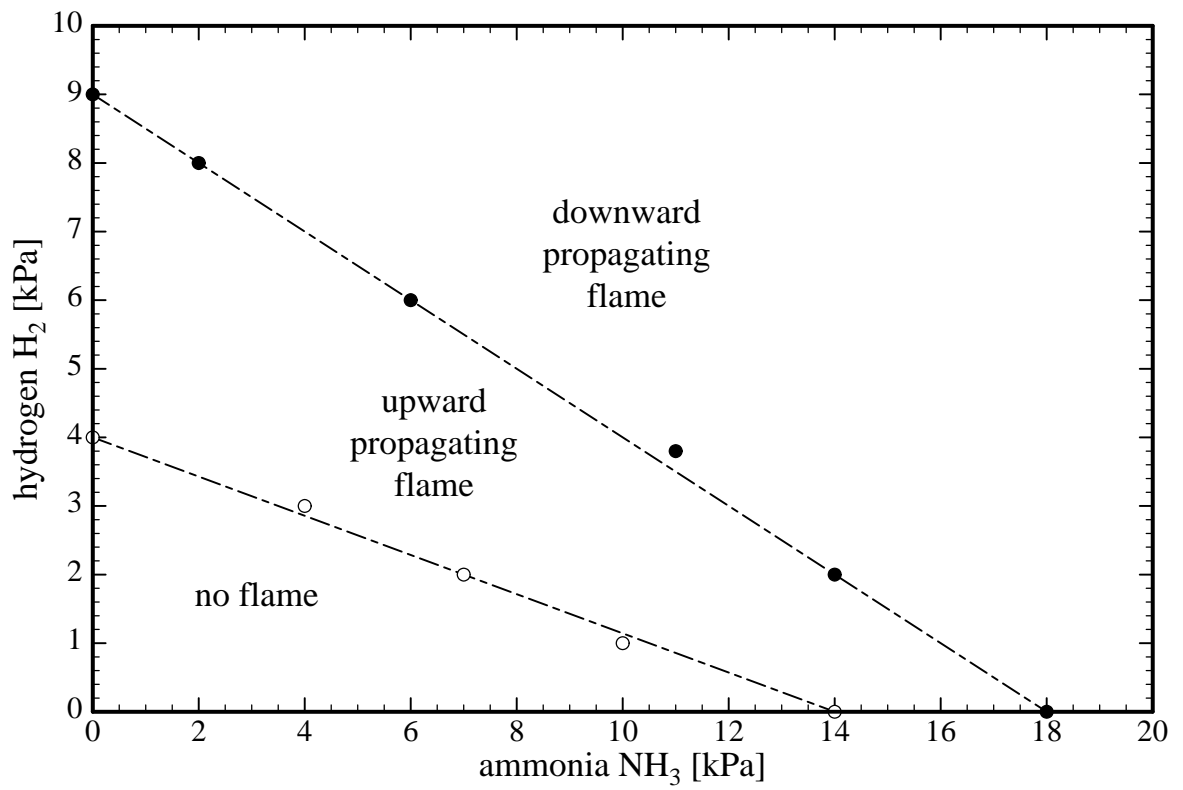


Figure 13:

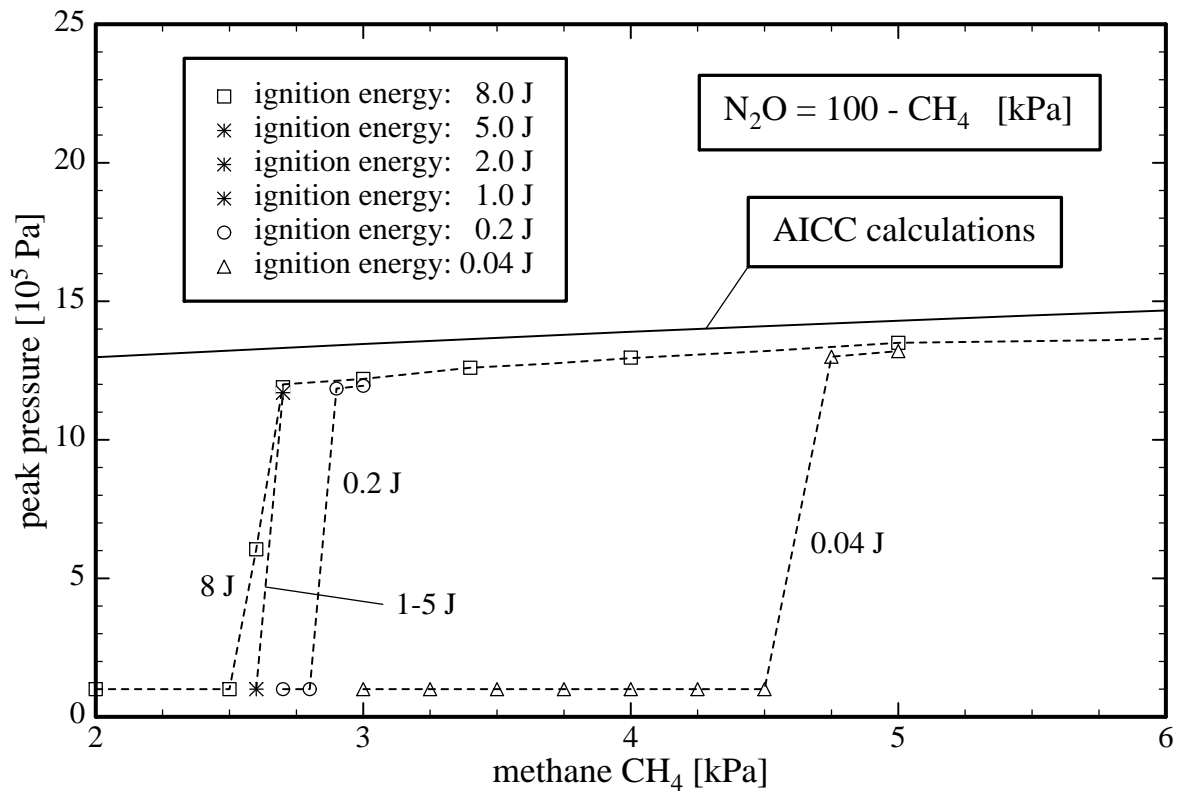


Figure 14:

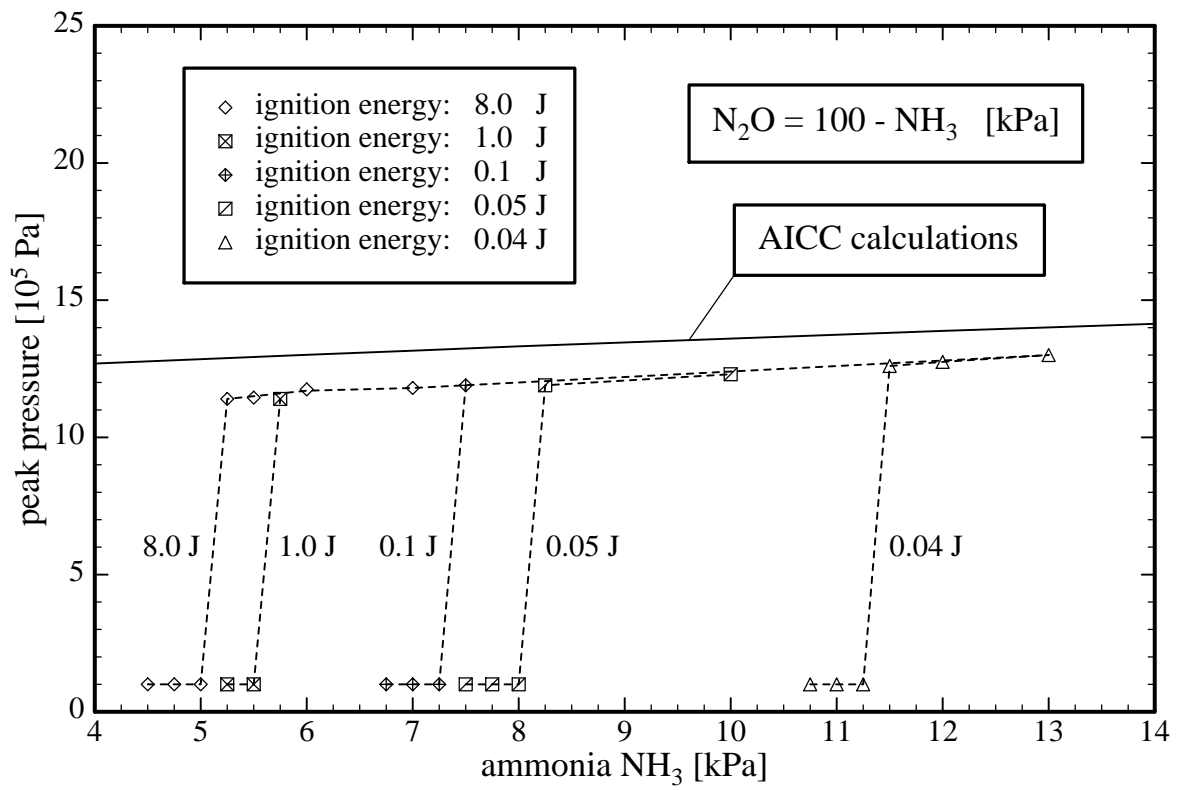


Figure 15:

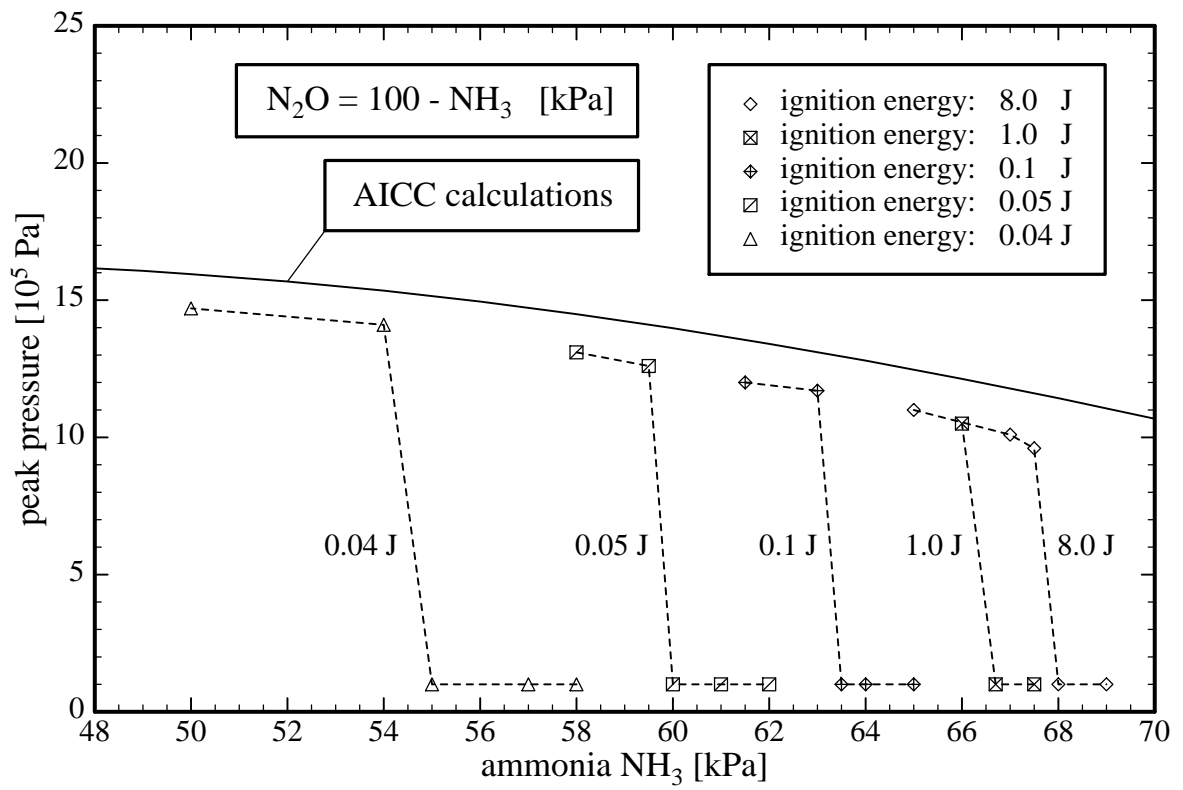


Figure 16:

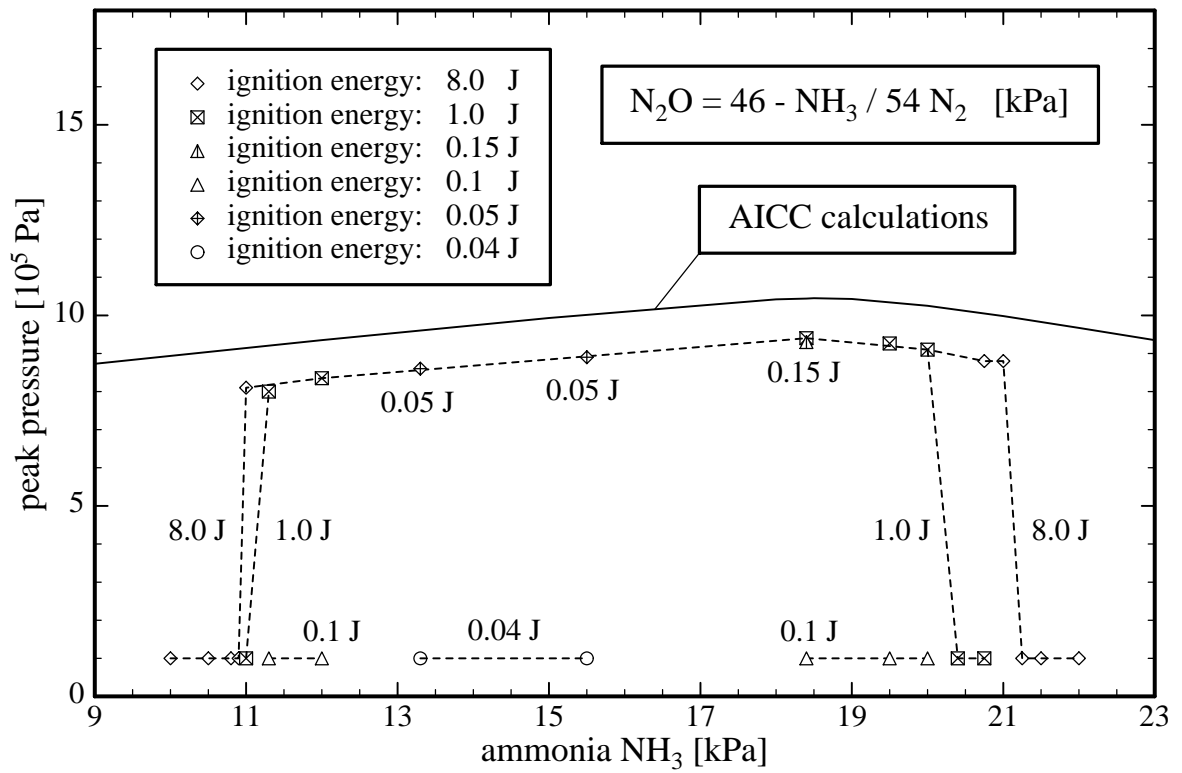


Figure 17:

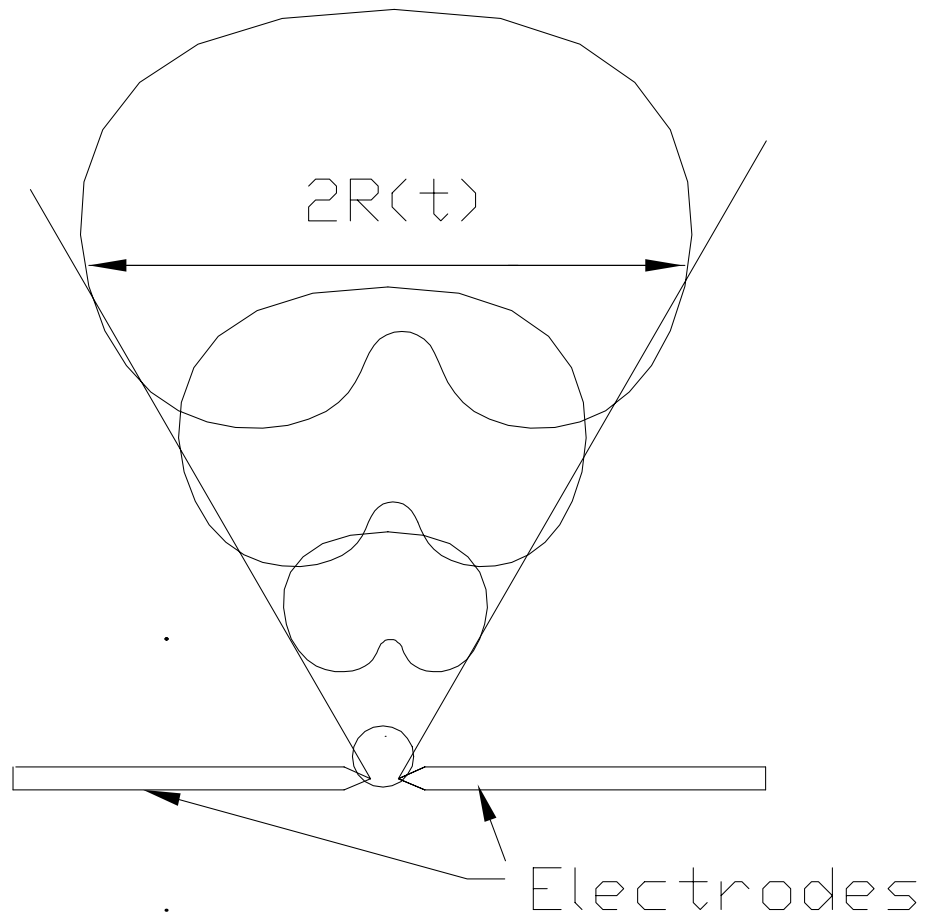


Figure 18:

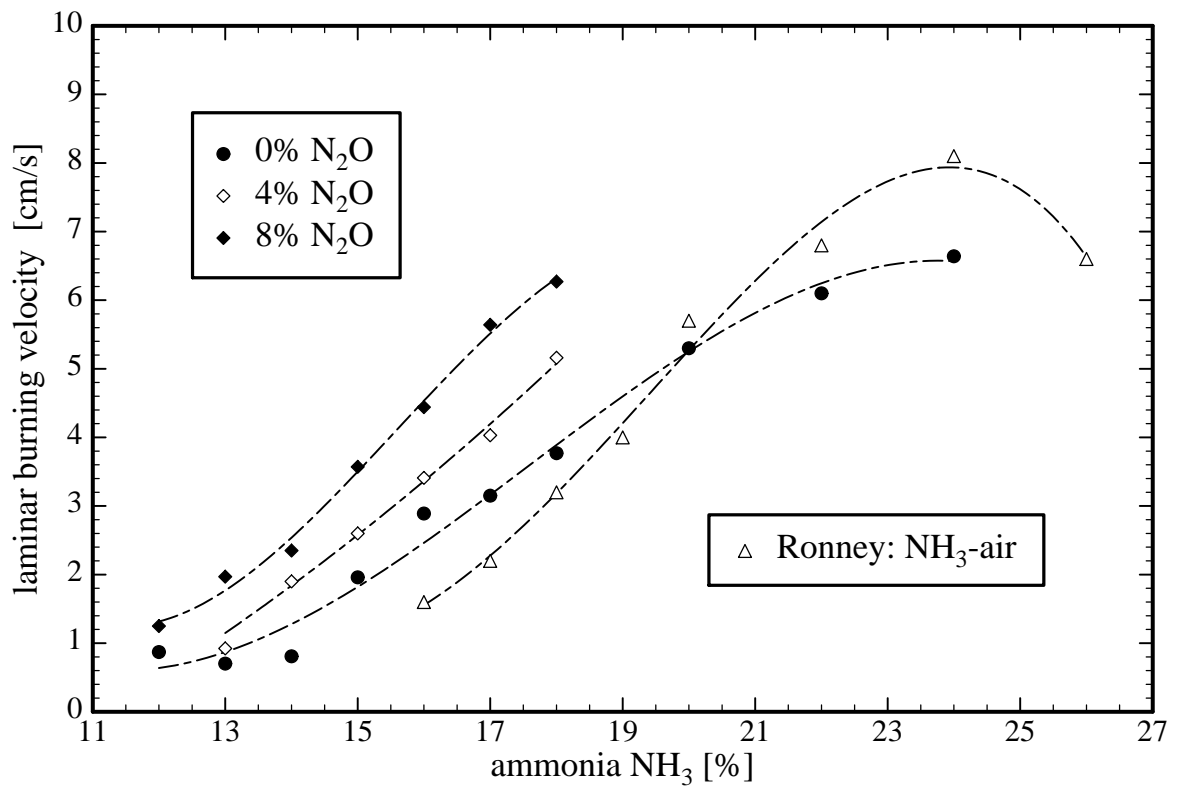


Figure 19:

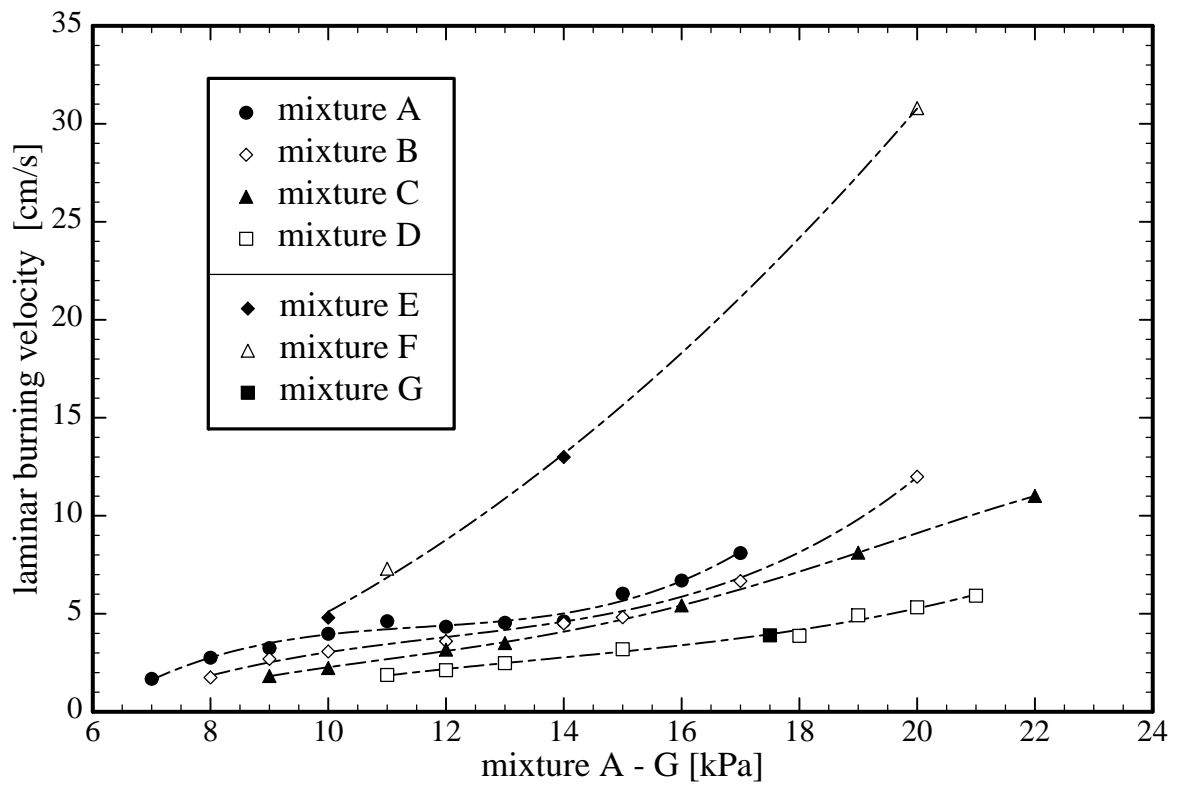


Figure 20: